Cell



# Divergent sensory pathways of sneezing and coughing

## Graphical abstract

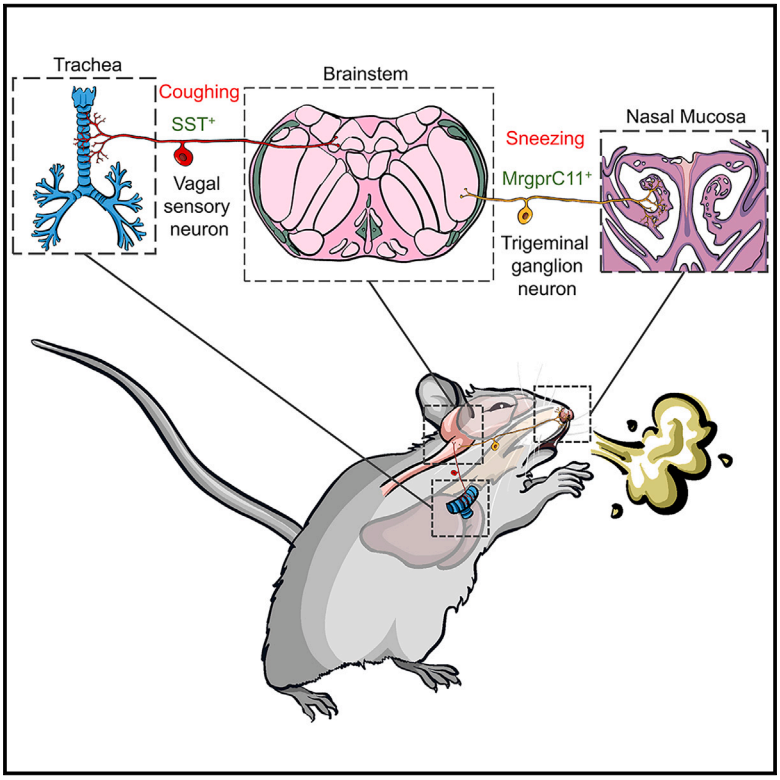


## Authors

Haowu Jiang, Huan Cui, Mengyu Chen, ..., Kangyun Wu, Michael J. Holtzman, Qin Liu

## Correspondence

qinliu@wustl.edu

## In brief

Sneezing and coughing are frequently associated with allergies and respiratory viral infections. This study reveals that sneezing and coughing are initiated by discrete sensory receptors and transmitted by divergent neuropathways, offering drug targets for managing pathological sneezing and coughing.

## Highlights

- Sneezing and coughing are mediated by distinct sensory populations
- Nasal MrgprC11-expressing sensory neurons serve as a core "sneeze" population
- Airway SST-expressing sensory neurons mediate chemically induced cough
- Sneezing and coughing are transmitted and modulated by divergent neuropathways

Jiang et al., 2024, Cell *187*, 5981–5997
October 17, 2024 
https://doi.org/10.1016/j.cell.2024.08.009

CellPress

Cell

CellPress
OPEN ACCESS

Article

# Divergent sensory pathways of sneezing and coughing

Haowu Jiang,[1,4] Huan Cui,[1,4] Mengyu Chen,[1] Fengxian Li,[1] Xiaolei Shen,[1] Changxiong J. Guo,[1] George E. Hoekel,[1] Yuyan Zhu,[2] Liang Han,[2] Kangyun Wu,[3] Michael J. Holtzman,[3] and Qin Liu[1,5,*]

[1]Department of Anesthesiology, Washington University Pain Center, Washington University School of Medicine in St. Louis, St. Louis, MO 63110, USA

[2]The School of Biological Sciences, Georgia Institute of Technology, Atlanta, GA 30332, USA

[3]Pulmonary and Critical Care Medicine, Washington University School of Medicine in St. Louis, St. Louis, MO 63110, USA

[4]These authors contributed equally

[5]Lead contact

*Correspondence: qinliu@wustl.edu

https://doi.org/10.1016/j.cell.2024.08.009

## SUMMARY

Sneezing and coughing are primary symptoms of many respiratory viral infections and allergies. It is generally assumed that sneezing and coughing involve common sensory receptors and molecular neurotransmission mechanisms. Here, we show that the nasal mucosa is innervated by several discrete populations of sensory neurons, but only one population (MrgprC11$^{+}$MrgprA3$^{-}$) mediates sneezing responses to a multitude of nasal irritants, allergens, and viruses. Although this population also innervates the trachea, it does not mediate coughing, as revealed by our newly established cough model. Instead, a distinct sensory population (somatostatin [SST$^{+}$]) mediates coughing but not sneezing, unraveling an unforeseen sensory difference between sneezing and coughing. At the circuit level, sneeze and cough signals are transmitted and modulated by divergent neuropathways. Together, our study reveals the difference in sensory receptors and neurotransmission/modulation mechanisms between sneezing and coughing, offering neuronal drug targets for symptom management in respiratory viral infections and allergies.

## INTRODUCTION

Respiratory viral infections (e.g., influenza, common cold, and COVID-19) frequently induce sneezing and coughing by activating primary sensory fibers innervating the nose and lower airways, respectively. Presumptively designed as host defense mechanisms, sneezing and coughing are believed to protect the airway by ejecting pathogens, allergens, and irritants. However, these two reflexes may also be hijacked by respiratory viruses for spreading to new hosts. In fact, respiratory infections are most commonly transmitted via virus-containing aerosol droplets generated by sneezing or coughing.[1–3]

Sneezing is evoked by primary sensory fibers that innervate the nasal mucosa. The nasal mucosa is densely innervated by the peripheral axons of diverse sensory neurons located in the trigeminal ganglia. These neurons detect mechanical, thermal, and chemical stimuli via membrane ion channels or receptors on their peripheral axons and transmit signals via their central axons to the brainstem. Electrical stimulations of the ethmoidal nerve (comprising nasal sensory fibers) trigger the sneezing reflex.[4,5] However, primary sensory neurons display a high degree of heterogeneity in terms of axonal innervation patterns, gene expression, physiological properties, and functionalities.[6] It remains uncertain which population(s) of nasal sensory fibers within the ethmoidal nerves mediate sneezing. Moreover, sneezing can be evoked by respiratory viruses, allergens, and irritants that induce various nasal sensations (e.g., pain and itch) in humans.[7–9] This raises the further question of whether different nasal stimuli induce sneezing through discrete populations of nasal sensory neurons or a common core population.

Similar to sneezing, coughing is a respiratory reflex characterized by the convulsive expulsion of air but mainly occurs in the lower airway. These two respiratory reflexes can be triggered by many common airway pathogens, allergens, and irritants (e.g., air flow, capsaicin, and histamine). Both reflexes serve as mechanisms to expel agents that might injure the airway. Hence, it is generally assumed that sneezing and coughing involve common sensory receptor(s). To test this assumption, it is critical to identify the sensory receptors that mediate sneezing and/or coughing. However, it is controversial whether mice have the cough reflex.[10–13] Studies suggest that mice lack the cough reflex based on the observation that anesthetized mice do not show cough-like responses to mechanical stimuli applied to the respiratory tract.[13] By contrast, recent studies show that inhalation of ammonia or sulfur dioxide induces cough-like responses in awake mice.[10,11,14] However, ammonia and sulfur dioxide irritate both the olfactory system and the upper and lower

airways, and induce broad respiratory changes, complicating the interpretation of these results.

In this study, we show that the nasal mucosa is innervated by multiple populations of sensory neurons, but *in vivo* functional screening reveals that only one population (MrgprC11$^+$ MrgprA3$^-$) mediates sneezing. Interestingly, the same population of sensory neurons also innervates the lower respiratory tract. By developing a model for cough research, we identified the characteristic respiratory and audio patterns of coughs in mice, which are distinct from those of sneezes. Influenza infection and chemically induced coughing, however, were not mediated by MrgprC11$^+$ neurons. Instead, a discrete sensory population (somatostatin [SST$^+$]) mediates coughing but not sneezing. Sneeze and cough signals are further transmitted and modulated by divergent central neuropathways. Our findings reveal an unanticipated sensory difference between sneezing and coughing, offering distinct neuronal targets for sneeze and cough management in respiratory infections and allergies.

## RESULTS

### The nasal mucosa is innervated by multiple populations of sensory neurons

To identify the neuronal populations that elicit sneezing, we first examined sensory innervation in the nasal mucosa. The respiratory epithelium lining the nasal turbinate and septum is densely innervated by primary sensory neurons.[15] Our study has shown that the transient receptor potential cation channel subfamily V member 1 (TRPV1) is broadly expressed by nasal sensory neurons and TRPV1$^+$ sensory neurons mediate chemically induced and allergy-associated sneezing.[15] Among the sensory populations examined, we found that four discrete populations of C-fiber sensory neurons innervate the nasal mucosa by genetic axonal tracing. The first population is MrgprD$^+$ polymodal C-fiber afferent neurons that mediate both mechanical pain and histamine-independent itch.[16–18] As revealed by *Mrgprd*$^{EGFPf/+}$ knockin reporter mice, MrgprD$^+$ sensory fibers innervate the anterior part of the nose (Figure 1A), but not the posterior part. Because sneezing can be mediated by sensory fibers in both the anterior and posterior parts of the nose,[19] this innervation pattern suggests either that MrgprD$^+$ neurons do not mediate sneezing or that sneezing occurring in the different parts of the nose involves distinct sensory populations.

The second population is SST$^+$ sensory neurons that express the receptors for serotonin and interleukin (IL)-31 and mediate itch evoked by these pruritogens.[20,21] This population also expresses the capsaicin-sensitive TRPV1 channel and histamine receptor.[20,21] SST$^+$ neurons innervate the nasal turbinate as revealed by genetic axonal tracing using *Sst*$^{Cre/+}$; *ROSA26*$^{tdTomato/+}$ (*Sst*$^{tdTomato}$) mice (Figure 1B). Sparse innervations were also observed in the septum and nasal wall (Figure 1B). In contrast to the dense innervation of nasal mucosa by TRPV1$^+$ sensory neurons,[15] SST$^+$ neuron innervation is relatively sparse and comprises a small subset of nasal TRPV1$^+$ sensory fibers. It is unknown whether they mediate sneezing among diverse subsets of TRPV1$^+$ neurons.

The third population is the transient receptor potential cation channel subfamily M member 8 (TRPM8)-expressing cold-sensing neurons. The TRPM8 channel can be activated by both cold and menthol (an active component of peppermint[22–25]). In humans, cold induces rhinorrhea but rarely sneezing.[26,27] As revealed by *Trpm8*$^{EGFPf/+}$ knockin reporter mice, TRPM8$^+$ sensory fibers sparsely innervate the epithelial lining of the nasal turbinate and septum (Figure 1C).

The fourth population is MrgprC11$^+$ sensory neurons. MrgprC11 is a G-protein-coupled receptor that has been reportedly involved in itch and pain modulation.[28–30] As revealed by *Mrgprc11*$^{CreERT2}$; *ROSA26*$^{tdTomato/+}$ mice (called *Mrgprc11*$^{tdTomato}$ after tamoxifen treatments), MrgprC11$^+$ sensory neurons densely innervate the mucosa of nasal wall, turbinate, and septum (Figure 1D). Interestingly, their innervation of the nasal turbinate is particularly high, which might underlie the super-sensitivity of the nasal turbinate to environmental irritants. Retrograde tracing of sensory neurons innervating the nasal mucosa indicated that MrgprC11$^+$ sensory neurons account for 17.08% ± 0.76% of total nasal sensory neurons (Figures S1A–S1D).

In addition to the nasal mucosa, the skin is innervated by MrgprC11$^+$ sensory neurons.[31] In skin sensory neurons, MrgprC11 expression largely overlaps with MrgprA3, an itch receptor that recognizes the anti-malaria drug chloroquine.[31,32] Strikingly, we failed to find any of MrgprA3-expressing sensory fibers in the nose using *Mrgpra3*$^{GFP\text{-}Cre}$; *ROSA26*$^{tdTomato/+}$ (*Mrgpra3*$^{tdTomato}$) mice (Figure 1E), suggesting that nasal MrgprC11$^+$ sensory neurons lack the expression of MrgprA3 (MrgprC11$^+$MrgprA3$^-$) and are different from their skin counterpart. Moreover, studies have indicated that a subset of MrgprC11$^+$ sensory neurons express MrgprB4,[33] a molecular marker for C-fiber tactile afferents neurons.[34–36] However, we did not detect MrgprB4-expressing sensory fibers in the nose using *Mrgprb4*$^{Cre\text{-}tdTomato/+}$ mice (Figure 1F). These results suggest that nasal MrgprC11$^+$ sensory neurons do not co-express MrgprA3 or MrgprB4 and are distinct from those innervating the skin. Their physiological function is therefore difficult to speculate.

To confirm the sensory innervation pattern of the nasal mucosa, we conducted retrograde labeling from the anterior ethmoidal nerve and single-cell quantitative reverse-transcription PCR (RT-qPCR). Correlating well with genetically guided axonal tracing, single-cell RT-qPCR showed the expression of *Mrgprd*, *Trpm8*, *Sst*, and *Mrgprc11* in retrogradely labeled nasal sensory neurons (Figure 1G). In contrast, no expression of *Mrgpra3* or *Mrgprb4* was detected, confirming that nasal MrgprC11$^+$ sensory neurons are distinct from those innervating the skin.[32,33,37] Further characterization indicates that nasal MrgprC11$^+$ neurons do not express most molecular markers of other sensory populations examined (Figures S1E an S1F), suggesting that they comprise a relatively homogeneous neuronal population at the transcriptional level.

### *In vivo* functional screening for the sneezing population(s)

To identify the nasal sensory population(s) that encode sneezing, we conducted *in vivo* functional screening by pharmacological or chemogenetic activation of various populations of

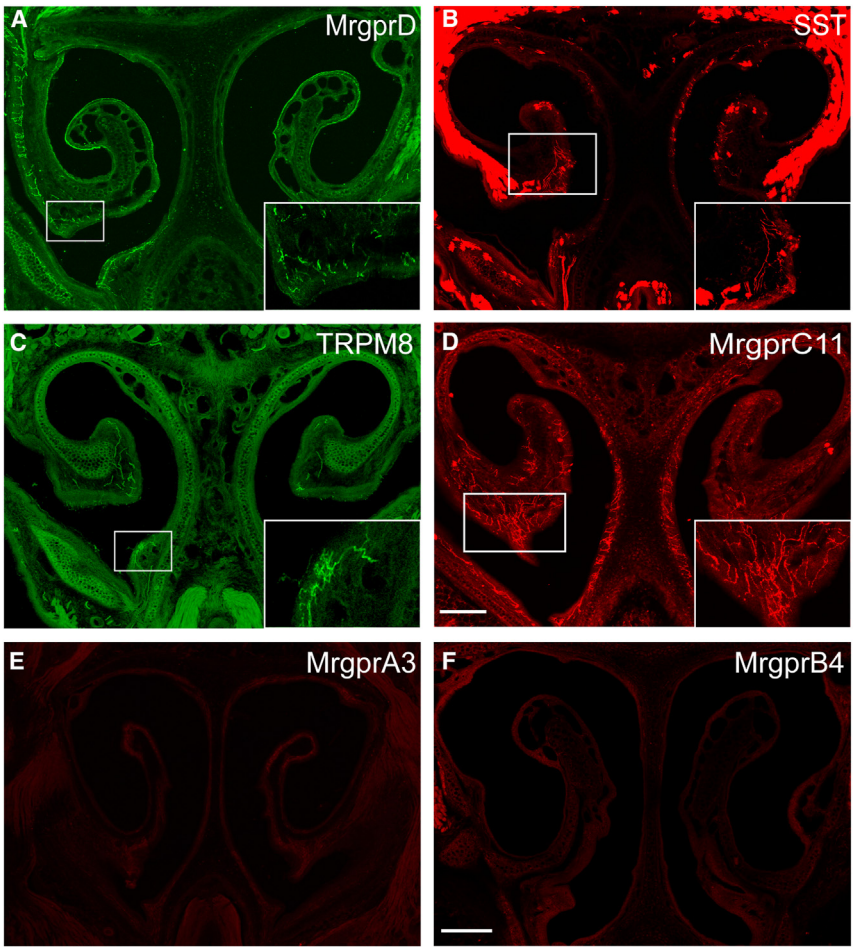


**Figure 1. The mouse nasal mucosa is innervated by multiple populations of sensory neurons**

(A) MrgprD-expressing polymodal C fibers (green) innervate the nasal turbinate and the septum in the nasal anterior region of *Mrgprd*$^{EGFPf/+}$ mice. The inset shows a higher-magnification view of the boxed area.

(B) Somatostatin (SST)-expressing itch-sensing fibers (red) innervate the nasal turbinate in *Sst*$^{Cre/+}$; *ROSA26*$^{tdTomato/+}$ mice.

(C) TRPM8-expressing cold-sensitive fibers (green) sparsely innervate the nasal turbinate and septum in *TRPM8*$^{EGFPf/+}$ mice.

(D) MrgprC11$^{+}$ sensory fibers (red) densely innervate the nasal wall, turbinate, and septum in *Mrgprc11*$^{CreERT2}$; *ROSA26*$^{tdTomato/+}$ mice. Notably, MrgprC11$^{+}$ innervation of the nasal turbinate is particularly high.

(E) MrgprA3-expressing itch-sensing fibers (red) do not innervate the nasal mucosa in *Mrgpra3*$^{GFP\text{-}Cre}$; *ROSA26*$^{tdTomato/+}$ mice.

(F) MrgprB4-expressing C-fiber tactile afferents (red) do not innervate the nasal mucosa in *Mrgprb4*$^{tdTomato\text{-}Cre/+}$ mice.

(G) Single-cell RT-qPCR of nasal sensory neurons retrogradely labeled from the anterior ethmoidal nerve. Each dot represents one sensory neuron. All images shown are representative of three biological replicates. The scale bars represent 500 μm.

See also Figure S1 and Table S1.

nasal sensory neurons (Figure 2A). We first activated nasal MrgprD$^{+}$ sensory neurons using β-alanine, a muscle-building supplement with the side effect of itch and tingling via activating MrgprD.[18,38] β-alanine failed to elicit significant sneezing responses compared with the vehicle control (Figure 2B), arguing against the involvement of the MrgprD population in sneezing. To confirm this finding, we further examined the behavioral consequence of activating MrgprD$^{+}$ neurons using a chemogenetic approach. We generated *Mrgprd*$^{CreERT2/+}$; *Tg*$^{CAG\text{-}LSL\text{-}Gq\text{-}DREADD(hM3Dq)}$ (*Mrgprd-M3*) mice by crossing *Mrgprd*$^{CreERT2/+}$ mice[39] with *Tg*$^{CAG\text{-}LSL\text{-}Gq\text{-}DREADD(hM3Dq)}$ mice. The specific expression of the *hM3Dq* transgene by MrgprD$^{+}$ trigeminal neurons in *Mrgprd-M3* mice was confirmed by RNAscope *in situ* hybridization (Figures S2A and S2B). Further electrophysiological recording showed that activation of the artificial G protein-coupled receptor (GPCR) hM3Dq using clozapine-N-oxide (CNO, an hM3Dq ligand[40]) induced action potential firings in MrgprD$^{+}$ neurons (Figures S2C and S2D). Finally, we activated nasal MrgprD$^{+}$ sensory fibers in these mice by nasal application of CNO. Consistent with the β-alanine assay, chemogenetic activation of MrgprD$^{+}$ neurons using CNO failed to elicit significant sneezing (Figure 2C), confirming the dispensable role of this population in sneezing. As a control, intradermal injection of CNO induced itch-related scratching behavior (Figure S2E) as well as pain-related wiping behavior shown by our recent study,[41] validating this chemogenetic approach *in vivo*.

We next examined the role of SST$^{+}$ neurons in sneezing. 5-hydroxytryptamine (serotonin) receptor 1F (5HT1F) agonist Ly344864 selectively activates SST$^{+}$ neurons and evokes itch in the skin.[21] However, this molecule failed to elicit significant sneezing responses (Figure 2D), suggesting that SST$^{+}$ neurons do not mediate sneezing. To confirm this result, we

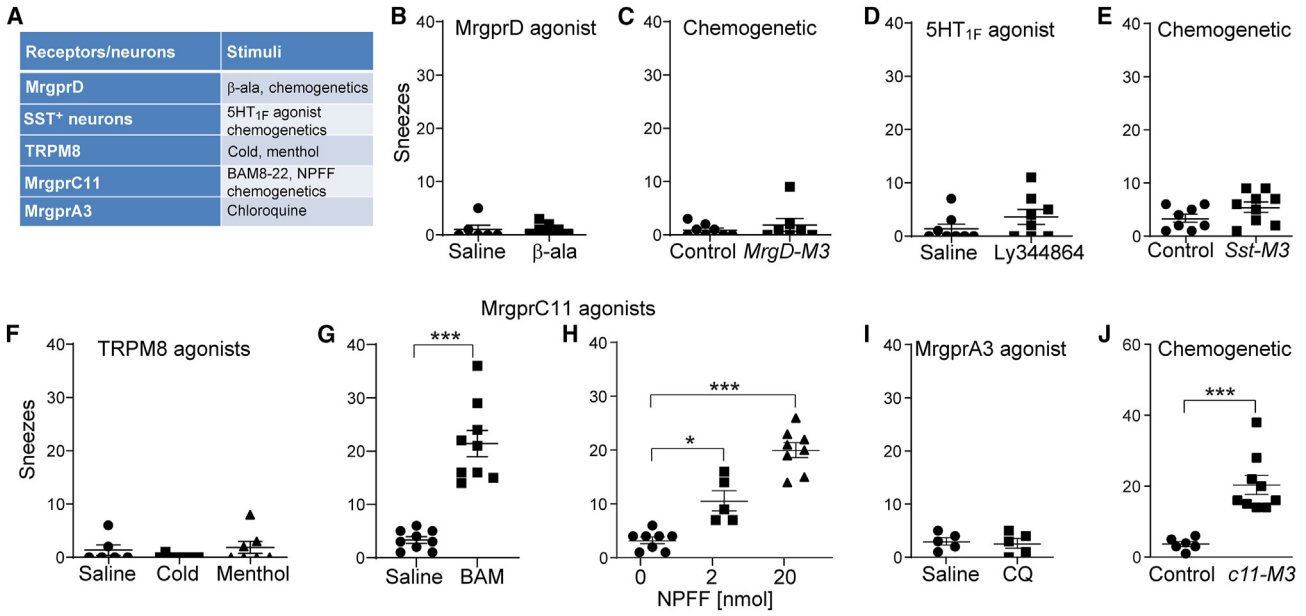


**Figure 2. *In vivo* functional screening for the neuronal population(s) mediating sneezing**

(A) Specific agonists for various populations of nasal sensory neurons.

(B) Aerosolized β-alanine solution (a specific agonist for MrgprD, 100 mM) did not elicit significant sneezing in WT mice compared with the vehicle control saline.

(C) Nasal application of clozapine-N-oxide (CNO, 2 nmol in 2 μL/nostril) did not elicit significant sneezing responses in $MrgprD^{CreERT2/+}$; $Tg^{CAG\text{-}LSL\text{-}Gq\text{-}DREADD(hM3Dq)}$ (*MrgprD-M3*) mice compared with littermate control mice.

(D) Aerosolized LY344864 solution (a $5HT_{1F}$ agonist that selectively activates $SST^+$ neurons, 1 mM) did not elicit significantly more sneezing than saline (vehicle control) in WT mice.

(E) Nasal application of CNO (2 nmol in 2 μL/nostril) did not elicit significant sneezing responses in $Sst^{Cre/+}$; $Tg^{CAG\text{-}LSL\text{-}Gq\text{-}DREADD(hM3Dq)}$ (*SST-M3*) mice compared with littermate control $Sst^{Cre/+}$ mice.

(F) Neither cold air (10°C) nor aerosolized menthol solution (a TRPM8 agonist, 1 mM) induced significant sneezing in WT mice.

(G and H) Nasal application of MrgprC11 agonists BAM 8-22 peptide (20 nmol in 2 μL/nostril) or NPFF peptide (2 and 20 nmol in 2 μL/nostril) elicited significant sneezing responses in WT mice compared with saline control.

(I) Aerosolized chloroquine solution (a specific agonist for MrgprA3, 12 mM) did not elicit significant sneezing compared with the vehicle control (saline) in WT mice.

(J) Nasal application of CNO (2 nmol in 2 μL/nostril) induced significant sneezing in $Mrgprc11^{CreERT2}$; $Tg^{CAG\text{-}hM3Dq\text{-}mCitrine}$ mice (*c11-M3*) compared with control $Mrgprc11^{CreERT2}$ mice. Each dot represents an individual mouse tested ($n$ = 5–11 mice/group). Data are presented as mean ± SEM. * $p \leq 0.05$; *** $p \leq 0.001$. See also Figures S2, S3, and S4.

generated $Sst^{cre/+}$; $Tg^{CAG\text{-}LSL\text{-}Gq\text{-}DREADD(hM3Dq)}$ (*Sst-M3*) mice. RNAscope *in situ* hybridization and electrophysiological recording confirmed the specific and functional expression of *hM3Dq* by $SST^+$ trigeminal neurons in *Sst-M3* mice (Figures S3A–S3D). However, chemogenetic activation of nasal $SST^+$ sensory fibers using CNO did not elicit significant sneezing (Figure 2E). In contrast, intradermal injection of CNO induced itch-related scratching behavior in *Sst-M3* mice (Figure S3E).

We further examined the role of $TRPM8^+$ cold-sensing neurons in sneezing. We found that activation of TRPM8 using cold air or menthol failed to elicit significant sneezing responses compared with the control group (Figure 2F), arguing against the involvement of TRPM8 in sneezing. This is consistent with clinical observations that people rarely sneeze upon exposure to cold air or mint.[26,27]

Finally, we examined the involvement of $MrgprC11^+MrgprA3^-$ sensory neurons in sneezing. We first examined the sneezing response to Bovine Adrenal Medulla (BAM) 8-22 peptide, an MrgprC11-specific agonist.[42,43] Remarkably, BAM induced significant sneezing in wild-type (WT) mice compared with vehicle control (Figure 2G). Furthermore, Neuropeptide FF (NPFF), an MrgprC11-activating neuropeptide released from mast cells,[44] also induced sneezing in a dose-dependent manner (Figure 2H). As a control, chloroquine, the agonist for MrgprA3, failed to evoke significant sneezing (Figure 2I), consistent with our observation that nasal $MrgprC11^+$ sensory neurons lack MrgprA3 expression. To further demonstrate that $MrgprC11^+$ sensory neurons mediate sneezing, we generated $Mrgprc11^{CreERT2}$; $Tg^{CAG\text{-}LSL\text{-}Gq\text{-}DREADD(hM3Dq)}$ (*Mrgprc11-M3*) mice. The specific and functional expression of *hM3Dq* by $MrgprC11^+$ trigeminal neurons in *Mrgprc11-M3* mice was confirmed by RNAscope *in situ* hybridization and electrophysiological recording (Figure S4). In contrast to *Mrgprd-M3* and *Sst-M3* mice, chemogenetic activation of nasal $MrgprC11^+$ sensory fibers using CNO induced significant sneezing behavior in *Mrgprc11-M3* mice (Figure 2J), demonstrating that $MrgprC11^+$ sensory neurons mediate sneezing. Our results indicate that among the sensory populations tested, nasal $MrgprC11^+MrgprA3^-$ sensory neurons mediate sneezing.

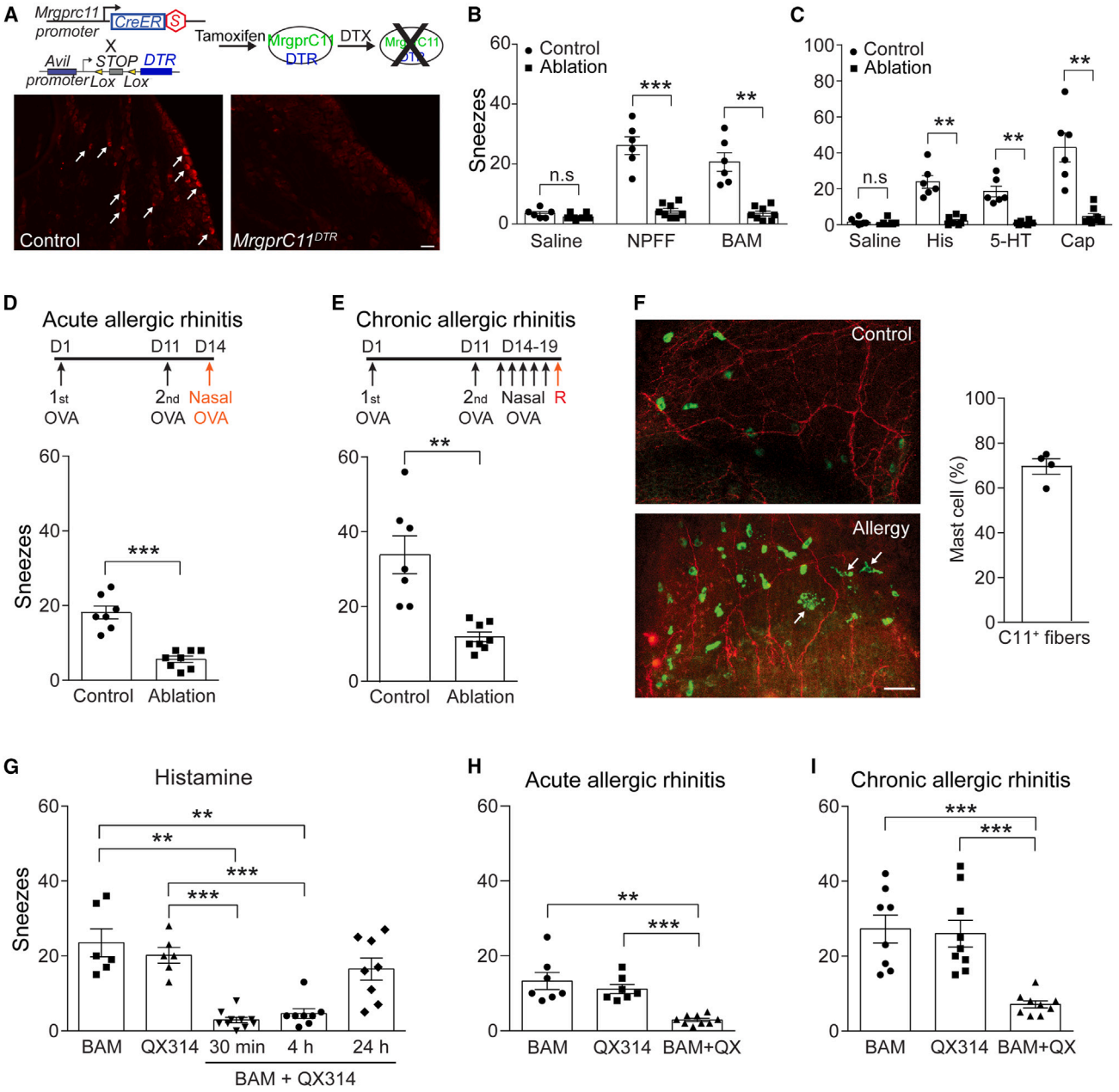


**Figure 3. Nasal MrgprC11$^{+}$ sensory neurons comprise a core sneeze population**

(A) Genetic ablation of MrgprC11$^{+}$ sensory neurons. Diagram showing the genetic strategy for specific ablation of MrgprC11$^{+}$ sensory neurons. Representative images show that MrgprC11$^{+}$ sensory neurons were ablated by diphtheria toxin (DTX) in the trigeminal ganglia from tamoxifen-treated *Mrgprc11$^{CreERT2}$; Avil$^{iDTR}$* mice (called *MrgprC11$^{DTR}$* mice), but not from control *Avil$^{iDTR}$* mice (indicated by arrows), as revealed by immunostaining for MrgprC11.

(B) Genetic ablation of MrgprC11$^{+}$ sensory neurons abolished the sneezing responses to MrgprC11 agonists NPFF (20 nmol in 2 μL/nostril) and BAM 8-22 (20 nmol in 2 μL/nostril) compared with control *Avil$^{iDTR}$* mice.

(C) Sneezing responses to aerosolized histamine solution (His, 100 mM), serotonin (5-HT, 1 mM), and capsaicin (Cap, 12 μM) were virtually abolished in MrgprC11$^{+}$ neuron-ablated mice compared with control *Avil$^{iDTR}$* mice.

(D and E) In the mouse models of acute and chronic allergic rhinitis, sneezing responses to allergen (ovalbumin, 0.2 mg in 2 μL PBS/nostril) challenge was significantly reduced in MrgprC11$^{+}$ neuron-ablated mice compared with control *Avil$^{iDTR}$* mice.

(F) Representative images of the whole-mount nasal mucosa from normal and allergic *Mrgprc11$^{CreERT2}$; ROSA26$^{tdTomato/+}$* mice. Note the accumulation and degranulation of avidin-stained mast cells (green, indicated by arrows) in the allergic mice. The bar graph shows the proportion of mast cells closely associated with MrgprC11$^{+}$ sensory fibers (red) in allergic mice ($n$ = 4 nasal mucosa explants).

*(legend continued on next page)*

## Nasal MrgprC11$^+$ sensory neurons comprise a core sneeze population

Sneezing can be evoked by a range of sensory stimuli that induce varying sensations in humans. For instance, capsaicin (a pungent compound from chili pepper) evokes intense burning pain and sneezing, whereas histamine and serotonin cause itch and sneezing.[7–9] Interestingly, nasal MrgprC11$^+$ sensory fibers are sensitive to a number of sneeze-inducing stimuli (e.g., capsaicin, histamine, and serotonin) and are insensitive to tested chemicals that do not induce sneezing (Figure S5). We therefore hypothesize that various sneeze-inducing stimuli activate a common population of nasal sensory neurons (i.e., MrgprC11$^+$) to trigger the sneezing reflex, even though they may activate other sensory neurons to elicit distinct sensations. To test our hypothesis, we examined whether genetic ablation of MrgprC11$^+$ neurons attenuates sneezing responses to a variety of chemical irritants. We generated *Mrgprc11$^{CreERT2}$; Avil$^{iDTR}$* mice by crossing *Mrgprc11$^{CreERT2}$* mice with Cre-dependent *Avil$^{iDTR}$* line.[21] After tamoxifen-induced Cre-*loxP* recombination, primate diphtheria toxin receptor (DTR) is specifically expressed in MrgprC11$^+$ sensory neurons (Figures 3A and S6). This line (called *Mrgprc11$^{DTR}$* after tamoxifen induction) enables us to ablate MrgprC11$^+$ neurons efficiently using diphtheria toxin (Figure 3A) and study the effects on sneezing. Remarkably, genetic ablation of MrgprC11$^+$ neurons virtually abolished sneezing responses to all tested irritants (Figures 3B and 3C), even though some chemical irritants (e.g., capsaicin, histamine, and serotonin) activate many other sensory neurons in addition to MrgprC11$^+$ neurons. Our results suggest that nasal MrgprC11$^+$ sensory neurons comprise a core population of "sneeze neurons" and broadly mediate sneezing.

Histamine, NPFF, and serotonin are released from mast cells upon degranulation and play essential roles in allergy.[44–49] We further examined whether MrgprC11$^+$ sensory neurons mediate sneezing associated with allergic rhinitis. Utilizing the mouse models of acute and chronic allergic rhinitis,[15] we found that ablation of MrgprC11$^+$ neurons significantly reduced allergic sneezing (Figures 3D and 3E). Whole-mount immunostaining revealed that most mast cells are closely associated with MrgprC11$^+$ sensory fibers in the nasal mucosa and release granules upon allergen challenge (Figure 3F).

Our data reveal that nasal MrgprC11$^+$ sensory neurons not only mediate nasal-irritant-induced sneezing but are also essential for allergy-associated pathological sneezing, providing a neuronal target for managing sneezing. To pharmacologically silence these neurons and test the effects on sneezing, we co-applied QX-314 with low-dose BAM to the mouse nasal cavity. QX-314 is a membrane-impermeable sodium-channel blocker. It can only enter nasal MrgprC11$^+$ sensory fibers through opened ion channels upon BAM-induced neuron excitation. This approach has been used broadly for targeted neuronal silencing in our and others' previous studies.[49,50] Silencing nasal MrgprC11$^+$ fibers using QX-314 with BAM not only abolished sneezing responses to histamine (Figure 3G) but also significantly suppressed sneezing associated with both acute and chronic allergic rhinitis (Figures 3H and 3I). Collectively, our study provides proof of concept for an anti-sneezing strategy by silencing nasal sneeze neurons.

## MrgprC11$^+$ sensory neurons mediate influenza-associated sneezing

Sneezing is a primary symptom of many types of respiratory viral infections, including the common cold, influenza, and COVID-19 (such as omicron variants). The mouse model of influenza infection has been widely used in virology, pulmonary, and immunological research. However, the study of influenza-associated sneezing is lacking. In the conventional mouse model of influenza infection, 25–40 μL viral solution is administered intranasally down to the lower respiratory tract and lung.[51–53] However, this model failed to generate significant sneezing, probably due to major infection of the lower airways. Because sneezing is caused by nasal infections, we developed a mouse model mimicking the upper airway infection of influenza by delivering a small volume of influenza virus to the nasal cavity. Because the viral volume is small (5 μL), influenza viral infection was confined to the nasal mucosa and pharynx, as revealed by viral transcript levels (Figure 4A). Immunostaining of influenza virus further confirmed a highly effective infection of the nasal mucosa but not the lower respiratory tract or lung (Figure 4B). As a negative control, UV-inactivated virus did not infect the nasal mucosa (Figure 4B).

In this model, the infected mice exhibited significant sneezing, which peaked at 36 h after viral inoculation (Figure 4C). Our model established that influenza infection induces sneezing in mice as in humans. As a negative control, mice inoculated with UV-inactivated virus did not sneeze (Figure 4C). Moreover, unlike the conventional mouse model for influenza infection,[51,53] mice lost body weight moderately and survived well in our model (Figure 4D). UV-inactivated virus induced significantly less body-weight loss (Figure 4D), confirming that body-weight loss resulted mainly from viral infection.

To determine the role of MrgprC11$^+$ sensory neurons in influenza-associated sneezing, we infected *Mrgprc11$^{DTR}$* mice and control *Avil$^{iDTR}$* littermates with influenza virus after tamoxifen and diphtheria toxin treatments. Remarkably, genetic ablation of MrgprC11$^+$ neurons almost abolished sneezing at 24- and 36-h after viral inoculation and significantly decreased sneezing at 48 h compared with control *Avil$^{iDTR}$* littermates (Figure 4E). Our result indicates that MrgprC11$^+$ neurons mediate influenza-associated sneezing.

(G) Sneezing responses induced by aerosolized histamine solution (100 mM) were inhibited by nasal application of QX-314 (1%, 2 μL) with BAM (2 nmol), compared with the control groups pretreated with either BAM (2 nmol in 2 μL) or QX-314 (1%, 2 μL) alone.
(H and I) In both acute and chronic allergic rhinitis models, allergen ovalbumin-induced sneezing responses were significantly suppressed by pretreatment of QX-314 (1%, 2 μL) with BAM (2 nmol) compared with the control groups pretreated with either BAM (2 nmol in 2 μL) or QX-314 (1%, 2 μL) alone. Each dot represents an individual mouse ($n$ = 6–11 mice/group). Data are presented as mean ± SEM. ** $p \leq 0.01$; *** $p \leq 0.001$; ns, not significant. All images shown are representative of at least three biological replicates. Scale bars, 50 μm.
See also Figures S5 and S6.

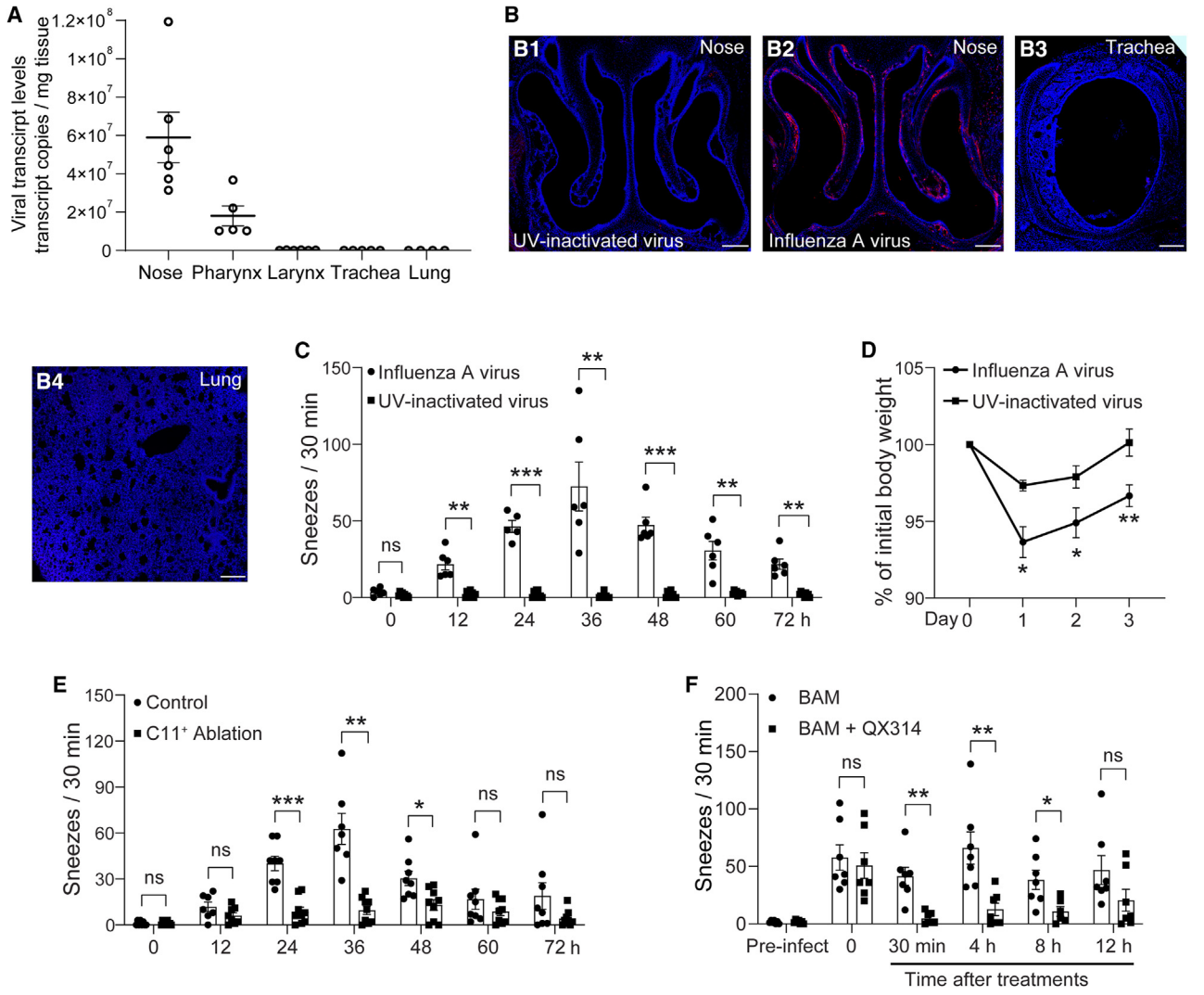


**Figure 4. MrgprC11$^+$ sensory neurons mediate influenza-associated sneezing**

(A) In our mouse model of influenza infection, influenza virus A/PR/8/34 mainly infected the nasal mucosa and pharynx, as revealed by digital PCR for viral transcript.

(B) Immunostaining shows the influenza viral infection (red) of the nasal mucosa (B2) but not the lower airway (trachea and lung, B3 and B4). As a negative control, UV-inactivated virus failed to infect the nasal mucosa (B1). Tissues were counterstained with DAPI (blue).

(C) Influenza-infected mice exhibited significant sneezing, which peaked at 36 h after viral inoculation. As a negative control, mice infected with UV-inactivated virus did not sneeze.

(D) Influenza-infected mice lost body weight moderately and survived well. As a control, UV-inactivated virus induced significantly less body-weight loss.

(E) Genetic ablation of MrgprC11$^+$ sensory neurons in *Mrgprc11$^{CreERT2}$; Avil$^{iDTR}$* mice significantly decreased influenza-associated sneezing compared with *Avil$^{iDTR}$* littermate controls.

(F) Pharmacological silencing of nasal MrgprC11$^+$ neurons with 1% QX-314 solution containing low-dose BAM (2 nmol in 2 μL; applied at 24 h after viral inoculation) significantly alleviated influenza-associated sneezing compared with controls treated with BAM (2 nmol in 2 μL) alone. Each dot represents an individual mouse tested ($n$ = 4–9 mice/group). Data are presented as mean ± SEM. * $p \leq 0.05$, ** $p \leq 0.01$, *** $p \leq 0.001$. All images shown are representative of three biological replicates. Scale bars, 200 μm.

Nasal MrgprC11$^+$ neurons provide a promising drug target for alleviating sneezing associated with respiratory viral infections. To silence these neurons, we co-applied QX-314 with low-dose BAM to the mouse nasal cavity 24 h after influenza virus inoculation. QX-mediated silencing of nasal MrgprC11$^+$ sensory fibers significantly attenuated influenza-induced sneezing (Figure 4F). The effect lasted for more than 8 h (Figure 4F). Therefore, pharmacological silencing of these neurons offers a novel and effective therapeutic strategy for managing sneezing during influenza infection.

## Establishment of a coughing model in mice

Our mouse influenza infection model induces a respiratory pattern other than sneezing, which is also characterized by

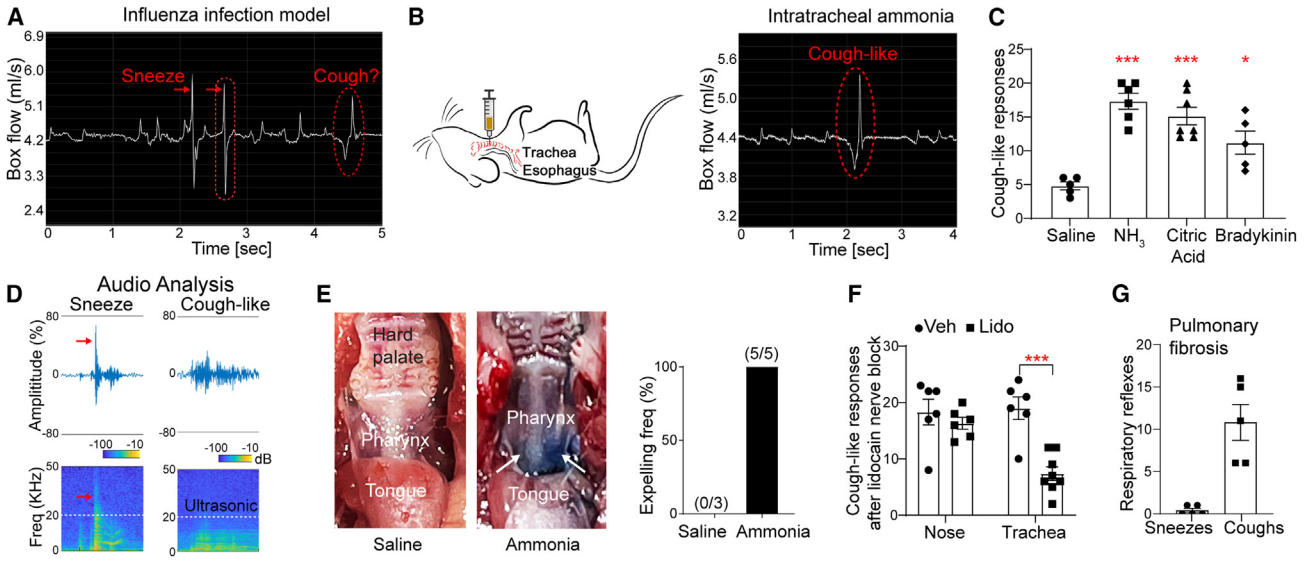


**Figure 5. Establishment of a coughing model in mice**

(A) Representative respiratory patterns of sneeze and cough-like responses in influenza-infected mice.

(B) Diagram showing a noninvasive intratracheal delivery approach. Intratracheal delivery of ammonia (0.2%, 10 μL) induced cough-like respiratory responses.

(C) Cough-like responses to intratracheal delivery of tussive agents, including ammonia (0.2%, 10 μL), citric acid (0.5 M, 10 μL), and bradykinin (25 μg in 10 μL). The vehicle saline control induced mild coughing via mechanical stimulation of the trachea.

(D) Representative audio patterns of sneeze and cough-like responses. The cough-like sound lacks sharp audio peaks observed in sneezing (indicated by an arrow). Audio spectrum analysis indicates that the sneeze sound displays many more ultrasonic components (indicated by an arrow) than the cough-like sound.

(E) Cough-like responses effectively expelled dye-containing ammonia solution from the trachea to the pharynx and mouth, as indicated by arrows ($n = 5$ mice). As a control, dye-containing saline does not induce such potent expelling (n = 3 mice).

(F) Lidocaine (1%) applied to the trachea, but not the nose, significantly reduced subsequent cough-like responses to intratracheal ammonia (0.2%, 10 μL).

(G) Pulmonary fibrosis after viral infection induces spontaneous coughing but not sneezing. Each dot represents an individual mouse tested ($n = 5$–8 mice/group).

Data are presented as mean ± SEM. * $p \leq 0.05$, *** $p \leq 0.001$. All images shown are representative of three biological replicates.

See also Video S1.

convulsive expulsion of air (Figure 5A). In addition to sneezing, coughing is a cardinal symptom of influenza infection in humans. In our mouse model, influenza infection of the pharynx was observed (see Figure 4A). It raises the questions of whether the respiratory pattern represents coughing in mice and whether MrgprC11$^+$ sensory neurons also mediate coughing.

The definition of cough is a sudden, forceful hacking sound to release air and clear an irritant from the throat (pharynx) or airway. We hypothesize that the pattern other than sneezing in the influenza infection model represents cough in mice. However, it is controversial whether mice can cough.[10–13] To test our hypothesis and determine whether mice cough, we developed a noninvasive procedure for delivering a small volume of test solution into the tracheas of mice lightly anesthetized by isoflurane (Figure 5B). Because the test solution is delivered directly into the trachea and bypasses the nasal cavity, this *new* approach minimizes the respiratory responses triggered by nasal sensory fibers (e.g., sneezing) or by olfaction. Furthermore, compared with conventional tracheotomy (a surgical procedure in which an incision is made in the front of the neck), our approach is noninvasive. Mice wake up immediately after the procedure, which allows the monitoring of respiratory responses in freely moving mice.

Studies have shown that ammonia, low PH, and bradykinin peptides elicit significant coughing in humans.[54–57] Tracheal delivery of these tussive agents indeed triggered the same respiratory pattern as in the influenza infection model (Figures 5B and 5C). Furthermore, the audio pattern of cough-like responses in mice is similar to that in humans.[58] The cough-like sound lacks sharp audio peak observed in sneezing (Figure 5D). Audio spectrum analysis indicates that the cough-like sound displays much less ultrasonic component than the sneeze sound (Figure 5D). Because coughing is an important mechanism for clearance of pathogens, allergens, and irritants from the throat and lower airway, we further examined the expelling effects of cough-like responses in mice. We found that dye-containing ammonia solution (tussive agent) was expelled from the trachea to the pharynx and mouth, whereas control saline did not induce such potent expelling (Figure 5E).

To confirm that the observed responses are coughs, we tested whether they are mediated by sensory fibers innervating the trachea rather than those in the nasal mucosa. To block nasal sensory fibers, we applied lidocaine, a local anesthetic, to the nasal cavity, as in a previous study.[11] We found that the cough-like responses to ammonia were not affected by nasal application of lidocaine (Figure 5F), confirming that these responses are not mediated by nasal sensory fibers. In contrast, local blockade of tracheal nerve fibers by lidocaine significantly reduced the cough-like responses to ammonia (Figure 5F).

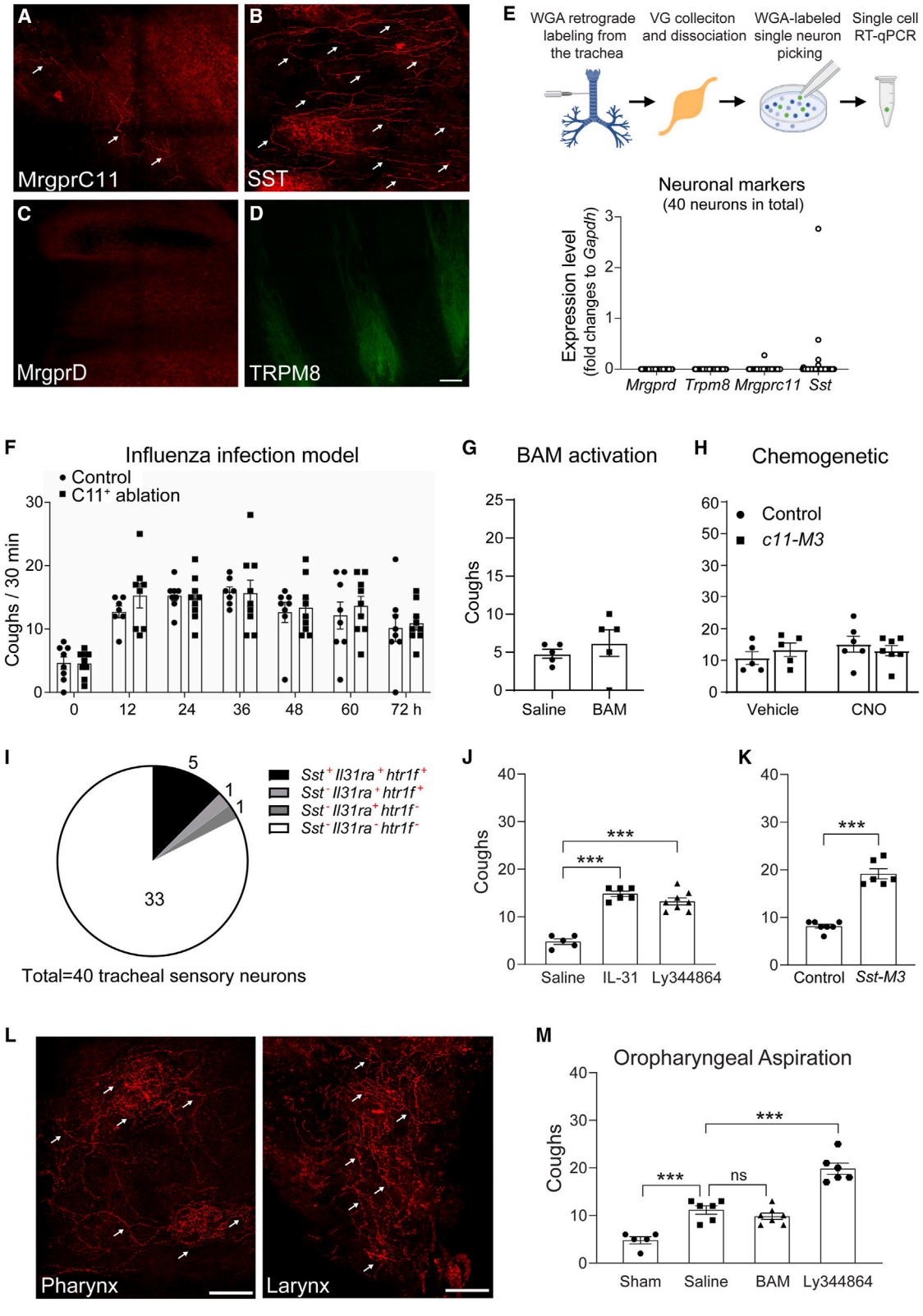


*(legend on next page)*

Respiratory viral infections frequently induce pulmonary fibrosis in both humans and animals, which induces chronic coughing.[59,60] Utilizing a pulmonary fibrosis model induced by viral infection, we found significant spontaneous coughing responses in mice (Figure 5G). In contrast, no significant sneezing was observed (Figure 5G). In summary, our results establish the existence of the cough reflex in mice, which is mediated by respiratory sensory fibers, characterized by convulsive expulsion of air, and essential for airway clearance.

## SST$^+$ sensory neurons but not MrgprC11$^+$ neurons mediate coughing

To screen for the sensory population(s) that mediate coughing, we examined the innervation of various afferent neuronal populations in the trachea. Among the sensory populations tested, we found that MrgprC11$^+$ sensory neurons innervate the trachea using both *Mrgprc11*$^{tdTomato}$ and *Mrgprc11*$^{CreER}$*; Rosa26*$^{PLAP/+}$ reporter lines (Figures 6A and S7). In addition, SST$^+$ sensory neurons densely innervate the trachea (Figures 6B and S7). By contrast, MrgprD$^+$ polymodal C-fiber afferent neurons and TRPM8$^+$ cold-sensing neurons do not innervate the trachea (Figures 6C and 6D), despite their innervation in the nasal mucosa (see Figure 1). The tracheal sensory innervation pattern was confirmed by retrograde tracing of airway vagal sensory neurons and single-cell RT-qPCR (Figure 6E). Our results reveal distinct sensory innervation patterns between the nose and lower airways.

To determine the role of MrgprC11$^+$ sensory neurons in coughing, we first examined influenza-associated coughing. Strikingly, influenza-induced coughing was not affected by genetic ablation of MrgprC11$^+$ sensory neurons (Figure 6F). To further investigate the role of MrgprC11$^+$ sensory neurons in coughing, we applied BAM peptide to the mouse trachea. Pharmacological activation of tracheal MrgprC11$^+$ sensory fibers by BAM failed to induce significant coughing responses compared with the vehicle control (Figure 6G). To confirm that MrgprC11$^+$ sensory neurons do not mediate coughing, we further examined the behavioral consequence of chemogenetic activation of tracheal MrgprC11$^+$ sensory fibers. Intratracheal application of CNO failed to induce significant coughing response in *Mrgprc11-M3* mice compared with either the vehicle control or *Mrgprc11*$^{CreERT2}$ littermate controls (Figure 6H). These results are in sharp contrast to our observation that nasal application of CNO induced significant sneezing behavior in *Mrgprc11-M3* mice (see Figure 2), demonstrating that MrgprC11$^+$ sensory neurons selectively mediate sneezing but not coughing.

In addition to MrgprC11$^+$ sensory neurons, SST$^+$ sensory neurons innervate the trachea. Although this population does not mediate sneezing (see Figure 2), do they mediate coughing? Studies have shown that SST$^+$ sensory neurons express the serotonin receptor 5HT1F and IL-31 receptor, and mediate itch evoked by 5HT1F agonist Ly344864 and IL-31 in the skin.[20,21] Single-cell RT-qPCR confirmed the expression of *Htr1f* and *Il31r* mRNA by tracheal SST$^+$ vagal neurons (Figure 6I). To probe the function of these neurons, we applied Ly344864 and IL-31 intratracheally to selectively activate SST$^+$ neurons innervating the trachea. Remarkably, both agents induced significant coughing in mice (Figure 6J). In addition to pharmacological activation, chemogenetic activation of tracheal SST$^+$ neurons induced significant coughing compared with the littermate controls (Figure 6K). These results indicate that SST$^+$ sensory neurons mediate coughing.

Because the tracheal innervations by MrgprC11$^+$ sensory neurons are less dense than those of SST$^+$ neurons, is it possible that tracheal MrgprC11$^+$ sensory neurons do not mediate coughing due to their innervation density? Coughing can be triggered by irritating the pharynx (throat) and larynx in addition to the trachea and lung. Strikingly, MrgprC11$^+$ sensory neurons densely innervate both the pharynx and larynx (Figure 6L). To activate

**Figure 6. SST$^+$ sensory neurons rather than MrgprC11$^+$ neurons mediate coughing**

(A and B) MrgprC11$^+$ and SST$^+$ sensory neurons innervate the trachea (indicated by arrows), as revealed by *Mrgprc11*$^{CreERT2}$*; ROSA26*$^{tdTomato/+}$ and *Sst*$^{Cre/+}$*; ROSA26*$^{tdTomato/+}$ reporter lines, respectively.

(C and D) MrgprD$^+$ polymodal C-fiber afferent neurons and TRPM8$^+$ cold-sensing neurons do not innervate the trachea, as revealed by *Mrgprd*$^{CreERT2/+}$*; ROSA26*$^{tdTomato}$ and *Trpm8*$^{EGFPf/+}$ reporter lines.

(E) Airway retrograde tracing and single-cell RT-qPCR confirmed the expression of *Mrgprc11* and *Sst* but no *Mrgprd* or *Trpm8* by airway vagal sensory neurons. Each dot represents an individual sensory neuron.

(F) Genetic ablation of MrgprC11$^+$ sensory neurons did not reduce influenza-associated coughing compared with *Avil*$^{iDTR}$ littermate controls.

(G) Intratracheal application of MrgprC11 agonist BAM 8-22 peptide (100 nmol in 10 μL) did not induce significantly more coughs than vehicle control (saline) in WT mice.

(H) Intratracheal application of CNO (10 nmol in 10 μL) did not induce significant coughing in *Mrgprc11*$^{CreERT2}$*; Tg*$^{CAG\text{-}hM3Dq\text{-}mCitrine}$ (*c11-M3*) mice compared with vehicle control and *Mrgprc11*$^{CreERT2}$ littermate controls.

(I) Single-cell RT-qPCR confirmed the expression of *Htr1f* and *Il31r* mRNA by tracheal SST$^+$ vagal neurons.

(J) Pharmacological activation of tracheal SST$^+$ neurons by LY344864 (a $5HT_{1F}$ agonist that selectively activates SST$^+$ neurons, 10 nmol in 10 μL) and IL-31 (0.04 nmol in 10 μL) induced significantly more coughs than vehicle control (saline).

(K) Chemogenetic activation of tracheal SST$^+$ neurons with CNO (10 nmol in 10 μL) induced significant coughing in *Sst*$^{Cre/+}$*; Tg*$^{CAG\text{-}hM3Dq\text{-}mCitrine}$ (*Sst-M3*) mice compared with *Sst*$^{Cre/+}$ littermate controls.

(L) MrgprC11$^+$ sensory fibers (red, indicated by arrows) densely innervate the whole-mount pharynx and larynx, as revealed by the *Mrgprc11*$^{CreERT2}$*; ROSA26*$^{tdTomato/+}$ reporter line.

(M) In a mouse model of oropharyngeal aspiration, aspiration of saline solution (25 μL) evoked significant coughing via mechanical stimulation of the airway. Aspiration of BAM 8-22 solution (250 nmol in 25 μL) did not induce more coughs than saline. As a positive control, aspiration of Ly344864 solution (25 nmol in 25 μL) induced significantly more coughs than saline. Each dot in (F)–(H), (J), (K), and (M) represents an individual mouse tested ($n$ = 5–9 mice/group). Data are presented as mean ± SEM. *** $p \leq 0.001$; ns, not significant. All images shown are representative of three biological replicates. Scare bars, 100 μm.

See also Figure S7.

pharyngeal and laryngeal sensory fibers, we utilized a mouse model for oropharyngeal aspiration in which the test solution is aspirated into the airway through forced mouth breathing.[61] In this model, aspiration of saline solution evoked significant mechanically induced coughing but no sneezing (Figure 6M), consistent with the observations of liquid aspiration in humans. However, aspiration of BAM solution did not induce more coughs than the saline control (Figure 6M). In contrast, aspiration of Ly344864 solution significantly increased coughing (Figure 6M). These results confirm that activation of airway MrgprC11$^+$ sensory fibers does not induce coughing. Collectively, our results unravel distinct sensory receptors mediating coughing and sneezing.

### Sneezing and coughing are mediated and modulated by divergent sensory pathways

Our previous study showed that nasal sensory neurons release neuromedin B (NMB) peptide to activate NMB receptor (NMBR)-expressing postsynaptic neurons in the brainstem's sneeze-evoking region for signaling sneezing.[15] In contrast, airway sensory neurons synapse in the nucleus tractus solitarius (NTS) to mediate coughing.[62] Although sneezing and coughing are encoded and transmitted by discrete anatomical pathways, do they have a common neurotransmission mechanism at the molecular level?

To address this question, we first confirmed that MrgprC11$^+$ sensory fibers anatomically and functionally synapse with most NMBR$^+$ neurons in the brainstem's sneeze-evoking region (Figures 7A and 7B). Although MrgprC11$^+$ sensory neurons represent a small subset of NMB-expressing trigeminal neurons (Figure S7), conditional knockout of *Nmb* in MrgprC11$^+$ neurons abolished sneezing responses to BAM and NPFF peptides (Figure 7C). These results indicate that nasal MrgprC11$^+$ sensory neurons release NMB peptide to activate NMBR$^+$ neurons within the central sneeze-evoking region for signaling sneezing. In contrast, retrograde tracing from the mouse airway reveals few to no NMBR-GFP neurons in the central projection zone of airway sensory neurons within the NTS (Figure 7D). Ablation of NMBR$^+$ NTS neurons using NMB-saporin did not affect the coughing responses to Ly344864 or IL-31 (Figure 7E), suggesting that NMB-sensitive NTS neurons do not mediate coughing.

Because SST$^+$ airway neurons mediate coughing, it is reasonable to speculate that a subset of their postsynaptic neurons within the NTS is sensitive to the neuropeptide SST and plays a role in coughing. To test our hypothesis, we performed microinjection of SST-saporin to the airway central projection zone within the NTS. Strikingly, ablation of SST-sensitive neurons significantly increased spontaneous coughing (Figure 7F), suggesting that these neurons have an inhibitory effect on cough signaling. Previous studies indicate that SST inhibits inhibitory dynorphin neurons (disinhibition) and promotes itch.[63,64] A similar mechanism may promote coughing. This SST-dependent modulatory neuropathway would be selective for coughing but not sneezing, as pharmacological and chemogenetic activation of nasal SST$^+$ neurons does not elicit significant sneezing (see Figure 2). In summary, our results unravel divergent sensory pathways of sneezing and coughing at the molecular and cellular levels.

## DISCUSSION

Sneezing and coughing are primary symptoms of many respiratory viral infections and allergies. They are defense mechanisms designed for expelling irritants, allergens, and pathogens from the nose and lower airways, respectively. In contrast to the popular assumption that sneeze and cough are triggered by common sensory receptors, we identified discrete sensory populations mediating sneezing and coughing, which differ in axon innervation patterns, molecular profiles, and functionalities. MrgprC11$^+$ sensory neurons densely innervate the nasal mucosa and mediate sneezing, whereas SST$^+$ neurons preferentially innervate the lower airways and mediate coughing. Furthermore, SST$^+$ neurons, instead of MrgprC11$^+$ neurons, selectively express the receptors for inflammatory mediators, such as IL-31 and cysteinyl leukotrienes,[20] and display unique sensitivity to airway inflammation. Studies have shown the upregulation of inflammatory mediators (e.g., IL-31 and leukotriene) in asthma and other pathological conditions.[65–67] It would be interesting to investigate the effects of chronic airway inflammation on the gene expression, axonal innervation, and neuronal excitability of SST$^+$ cough neurons. This will open a door to the study of pathological cough associated with asthma, long COVID, and chronic obstructive pulmonary disease (COPD).

From an evolutionary perspective, distinct sneeze and cough neuronal populations may provide complementary sensory surveillance and advantages in detection and physical clearance of potentially harmful substances. For example, many respiratory viruses (e.g., influenza, rhinovirus) induce both sneezing and coughing, but some respiratory viruses (e.g., early variants of severe acute respiratory syndrome coronavirus 2 [SARS-CoV-2] virus and respiratory syncytial virus [RSV]) mainly induce coughing.[68,69] The dual sensory surveillance by sneeze and cough neurons provides a broader and more efficient mechanism for detecting viral infections, especially when the virus escapes one sensory surveillance. This is particularly important as respiratory viruses evolve rapidly.

Translating our findings from mice to humans is important. With respect to MrgprC11$^+$ sneeze neurons, primate MrgprX1 is sensitive to MrgprC11 agonists and is the functional ortholog of mouse MrgprC11.[32,43,70] Interestingly, MrgprX1 is also selectively expressed by C-fiber sensory neurons in both humans and monkeys.[43,71] MrgprX1$^+$ neurons can be robustly activated by histamine in monkeys (unpublished data), suggesting the potential role of these neurons in sneezing. It would be interesting to study the innervation and physiological properties of MrgprX1$^+$ sensory fibers in human nasal mucosa under normal and pathological conditions. In addition, a transgenic mouse line was generated in which human MrgprX1 is expressed in mouse MrgprC11$^+$ sensory neurons while endogenous mouse Mrgprs were deleted.[72] This line enables us to study the function of hMrgprX1 receptor and hMrgprX1$^+$ neurons in a mouse model. Results from these studies will lay a solid foundation for studying and treating sneezing in humans.

For SST$^+$ cough neurons, similar translational studies will be conducted. Single-cell sequencing of human sensory neurons indicates that SST expression marks a neuronal cluster that also expresses the IL-31 receptor subunits (*IL31RA* and

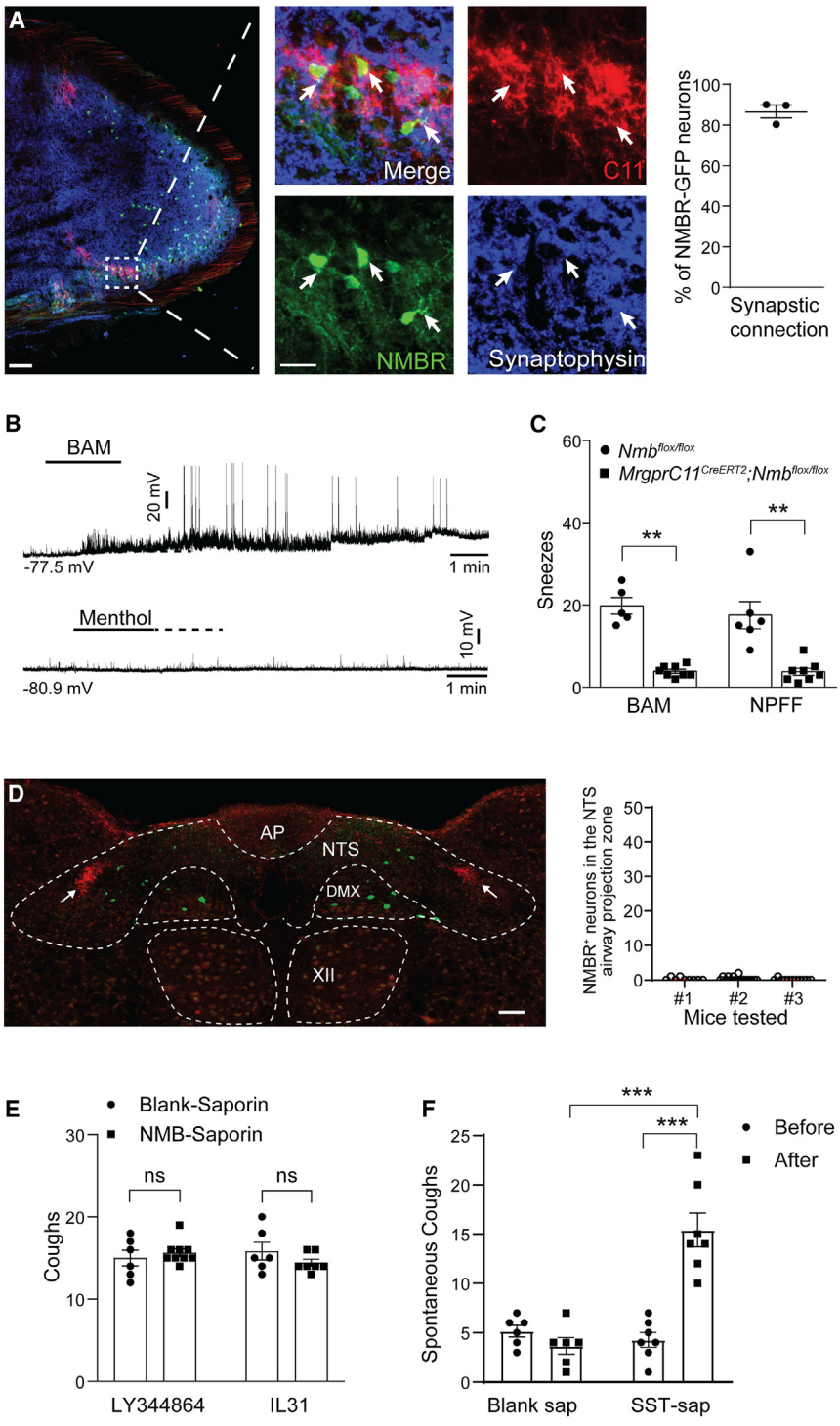


**Figure 7. Sneezing and coughing are mediated and modulated by divergent sensory pathways**

(A) Representative images showing that MrgprC11$^+$ afferents (red) express the presynaptic marker synaptophysin 1 (blue) and synapse with NMBR$^+$ neurons (green) in the brainstem's sneeze-evoking region. The synaptic connections were indicated by arrows in higher-magnification view of the boxed region. The graph shows the proportion of NMBR$^+$ neurons postsynaptic to MrgprC11$^+$ afferents in the sneeze-evoking region. Each dot represents an individual mouse ($n$ = 3).

(B) Representative traces showing that activation of MrgprC11$^+$ sensory neurons by BAM 8-22 peptide (100 μM) induced significant excitatory postsynaptic potentials (EPSPs) and led to action potential discharge in 7 out of 12 NMBR-GFP neurons recorded within the sneeze-evoking region. As a control, menthol (1 mM) activation of TRPM8$^+$ cold-sensing neurons failed to induce EPSP in NMBR-GFP neurons (0 out of 6 neurons recorded).

(C) *Mrgprc11*$^{CreERT2}$; *Nmb*$^{flox/flox}$ mice display significantly reduced sneezing responses to BAM (20 nmol in 2 μL saline) and neuropeptide FF (NPFF; 20 nmol in 2 μL saline).

(D) Representative coronal brainstem section of *Nmbr*$^{eGFP}$ mice showing that few to no NMBR-GFP neurons (green) in the central projection zone of airway sensory neurons (red, indicated by arrows) within the nucleus tractus solitarius (NTS), as revealed by retrograde tracing from the mouse airway using WGA-Alexa Fluor 555. The graph shows the number of NMBR-GFP neurons within the airway central projection zone (each dot represents a brainstem section). DMX: dorsal motor nucleus. XII: hypoglossal nucleus.

(E) Microinjection of NMB-saporin into the NTS did not significantly change the coughing responses to intratracheal delivery of LY344864 (10 nmol in 10 μL) or IL-31 (0.04 nmol in 10 μL).

(F) Microinjection of SST-saporin into the NTS induced significant spontaneous coughing compared with the blank saporin. Each dot in (C), (E), and (F) represents an individual mouse ($n$ = 5–9 mice/group). Data are presented as mean ± SEM. ** $p \leq 0.01$. *** $p \leq 0.001$; ns, not significant. All images shown are representative of three biological replicates. Scale bars, 100 μm.

See also Figure S7.

*OSMR*) and histamine receptors (*HRH1*), consistent with mouse and macaque SST$^+$ nociceptive/pruriceptive populations.[73–77] Different from mouse SST$^+$ neurons, however, human SST$^+$ neurons express the calcitonin gene-related peptide CGRP (*CALCA*) and the serotonin receptor *HTR3A* instead of *HTR1F* and do not express the cysteinyl leukotriene receptor 2 (*CYSLTR2*).[73–77] Characterization of SST$^+$ sensory fibers' innervation and physiological properties in human airway tissues under normal and disease conditions will help reveal their involvement in cough and advance our understanding of the neurobiology of cough in humans.

Targeting sneeze or cough neurons provides a safe and efficient strategy for symptom management in allergy and respiratory viral infections. First, because this strategy specifically silences a sensory population, it would not affect the functions

of other neuronal populations, goblet cells, glands, and airway epithelium. This will circumvent unwanted side effects that are commonly associated with conventional antihistamines or corticosteroids, including airway dryness, bleeding, and infections. Nasal or airway delivery of therapeutic reagents also minimizes systemic side-effects. Second, our proof-of-concept studies of silencing nasal sneeze neurons using a combination of BAM and QX-314 have yielded key pre-clinical evidence for the feasibility and effectiveness of this therapeutic strategy. The same strategy is applicable to managing cough. $SST^+$ cough neurons can be silenced by intratracheal delivery of QX-314 with SST-neuron-selective agonists such as Ly344864 in mice or HTR3A agonists in humans. Furthermore, human $SST^+$ neurons selectively express the receptor of IL-31, a cytokine involved in the pathophysiology of atopic dermatitis and other atopic disorders.[65] It would be interesting to investigate the roles of IL-31 and its receptor in cough. Clinical trials indicate that humanized anti-IL-31RA monoclonal antibody (CIM331, nemolizumab) significantly alleviates pruritus in patients with atopic dermatitis.[78,79] Because cough is frequently associated with airway itch or irritations,[80,81] the application of nemolizumab to pathological coughing could be exploited. Collectively, our studies reveal the neural basis of sneezing and coughing and identify drug targets for symptom management in allergies and respiratory viral infections.

## Limitations of the study

Cough can be elicited by both mechanical and chemical stimuli, which have been suggested to be detected by nodose Aδ fibers and bronchopulmonary C fibers, respectively.[62,82] Among diverse subsets of C-fiber neurons innervating the airway, our study identified a highly restricted subset of bronchopulmonary C fibers underlying chemically induced cough—the $SST^+$ airway sensory neurons. However, these neurons are unlikely to be the only neuronal population mediating cough. A study has shown that capsaicin desensitization of $TRPV1^+$ sensory fibers (including $SST^+$ fibers) abolished chemically induced coughing but did not affect mechanically induced coughing in guinea pigs.[83] Instead, mechanically induced coughing is likely mediated by nodose Aδ fibers.[62,82] Based on previous studies in guinea pigs, the nodose Aδ population is exquisitely sensitive to punctate mechanical stimuli,[62,82] which may underlie mechanically induced coughing associated with aspiration. Distinct from $SST^+$ C-fiber cough neurons, nodose Aδ fibers are insensitive to nociceptive stimuli such as bradykinin and capsaicin.[62,82] However, the molecular identity of these neurons remains elusive, hindering further molecular and genetic studies. It would be interesting to screen for Aδ cough neurons among diverse subsets of myelinated sensory neurons, using our cough behavioral models and mouse genetic tools, and further compare these with $SST^+$ C-fiber cough neurons in molecular profiles, physiological properties, functionalities, and circuits.

## RESOURCE AVAILABILITY

### Lead contact

Further information and requests for resources and reagents should be directed to and will be fulfilled by the lead contact, Qin Liu (qinliu@wustl.edu).

### Materials availability

The study did not generate new unique materials or reagents.

### Data and code availability

- This paper does not report nucleotide sequencing-associated datasets, proteomics, peptidomics, metabolomics, structures of biological macromolecules, or small-molecule crystallography.
- This paper does not report original code.
- Any additional information about the data reported in this paper is available from the lead contact upon request.

## ACKNOWLEDGMENTS

We thank Xinzhong Dong, Brian S. Kim, and Ru-Rong Ji for their insightful comments on the manuscript and Fengrui Zhang for helping with audio analysis. This work was supported by the National Institutes of Health, United States (grants R01AI163146, R01EY024704, and R01EY035261) and the Pew Scholar Award (to Q.L.). L.H. is supported by grant (R01HL141269) from the National Institutes of Health, United States. M.J.H. was supported by grants from the National Institutes of Health, United States (National Heart, Lung, and Blood Institute R35-HL145242; National Institute of Allergy and Infectious Diseases R01 AI130591; and Department of Defense TTDA W81XWH2010603 and W81XWH2210281).

## AUTHOR CONTRIBUTIONS

H.J. performed histochemistry study of nasal tissues, retrograde labeling from the anterior ethmoidal nerve (AEN), tissue and single-cell isolation for single-cell RT-qPCR and digital PCR, sneezing behavior study, *ex vivo* calcium imaging, whole-cell patch-clamp recordings, influenza infection model, whole-mount histochemistry staining, coughing behavior study, pulmonary fibrosis study, acute and chronic allergic rhinitis models, immunofluorescence staining of the sensory ganglia and the brainstem, brainstem slice preparation and electrophysiological recordings, and data analysis and participated in manuscript preparation and writing. H.C. performed histochemistry study of nasal tissues, retrograde labeling and genetic axonal tracings, single-cell RT-qPCR and digital PCR, sneezing behavior study, RNAscope *in situ* hybridization, influenza infection model, coughing behavior study, immunofluorescence staining of the sensory ganglia and the brainstem, and data analysis and participated in manuscript preparation. M.C. performed neuronal ablation with SST-saporin and NMB-saporin. F.L. performed retrograde labeling and genetic axonal tracings, immunofluorescence staining, sneezing behavior study, and data analysis. X.S. helped develop the influenza infection model and retrograde labeling from the AEN. C.J.G. performed single-cell RT-PCR, digital PCR, RNAscope *in situ* hybridization, and data analysis and participated in manuscript preparation and writing. G.E.H. performed digital PCR assay, data collection and analysis of sneezing behavior study, and RNAscope *in situ* hybridization. Y.Z. performed genetic axonal tracing in the trachea. L.H. helped characterize the transgenic mouse line MrgC11CreER, performed genetic axonal tracing, and participated in manuscript preparation. K.W. generated the pulmonary fibrosis model and participated in manuscript preparation. M.J.H. made intellectual contributions to sneezing and coughing studies and participated in manuscript preparation. Q.L. planned and directed all the experiments and wrote the paper.

## DECLARATION OF INTERESTS

M.J.H. has noncompeting financial interests unrelated to this work and is the Founder of NuPeak Therapeutics Inc.

## STAR★METHODS

Detailed methods are provided in the online version of this paper and include the following:

- KEY RESOURCES TABLE
- EXPERIMENTAL MODEL AND STUDY PARTICIPANT DETAILS

## SUPPLEMENTAL INFORMATION

Supplemental information can be found online at https://doi.org/10.1016/j.cell.2024.08.009.

Received: September 10, 2023
Revised: June 25, 2024
Accepted: August 7, 2024
Published: September 6, 2024

## REFERENCES

1. Bourouiba, L. (2020). Turbulent Gas Clouds and Respiratory Pathogen Emissions: Potential Implications for Reducing Transmission of COVID-19. JAMA *323*, 1837–1838. https://doi.org/10.1001/jama.2020.4756.
2. Tang, J.W., Li, Y., Eames, I., Chan, P.K., and Ridgway, G.L. (2006). Factors involved in the aerosol transmission of infection and control of ventilation in healthcare premises. J. Hosp. Infect. *64*, 100–114. https://doi.org/10.1016/j.jhin.2006.05.022.
3. Cole, E.C., and Cook, C.E. (1998). Characterization of infectious aerosols in health care facilities: an aid to effective engineering controls and preventive strategies. Am. J. Infect. Control *26*, 453–464. https://doi.org/10.1016/s0196-6553(98)70046-x.
4. Songu, M., and Cingi, C. (2009). Sneeze reflex: facts and fiction. Ther. Adv. Respir. Dis. *3*, 131–141. https://doi.org/10.1177/1753465809340571.
5. Wallois, F., Macron, J.M., Jounieaux, V., and Duron, B. (1991). Trigeminal afferences implied in the triggering or inhibition of sneezing in cats. Neurosci. Lett. *122*, 145–147.
6. Taylor-Clark, T.E., Kollarik, M., MacGlashan, D.W., Jr., and Undem, B.J. (2005). Nasal sensory nerve populations responding to histamine and capsaicin. J. Allergy Clin. Immunol. *116*, 1282–1288. https://doi.org/10.1016/j.jaci.2005.08.043.
7. Geppetti, P., Fusco, B.M., Marabini, S., Maggi, C.A., Fanciullacci, M., and Sicuteri, F. (1988). Secretion, pain and sneezing induced by the application of capsaicin to the nasal mucosa in man. Br. J. Pharmacol. *93*, 509–514.
8. Doyle, W.J., Boehm, S., and Skoner, D.P. (1990). Physiologic responses to intranasal dose-response challenges with histamine, methacholine, bradykinin, and prostaglandin in adult volunteers with and without nasal allergy. J. Allergy Clin. Immunol. *86*, 924–935.
9. Tønnesen, P., and Mygind, N. (1985). Nasal challenge with serotonin and histamine in normal persons. Allergy *40*, 350–353.
10. Lin, A.H., Hsu, C.C., Lin, Y.S., Lin, R.L., and Lee, L.Y. (2020). Mechanisms underlying the stimulatory effect of inhaled sulfur dioxide on vagal bronchopulmonary C-fibres. J. Physiol. *598*, 1093–1108. https://doi.org/10.1113/JP279152.
11. Zhang, C., Lin, R.L., Hong, J., Khosravi, M., and Lee, L.Y. (2017). Cough and expiration reflexes elicited by inhaled irritant gases are intensified in ovalbumin-sensitized mice. Am. J. Physiol. Regul. Integr. Comp. Physiol. *312*, R718–R726. https://doi.org/10.1152/ajpregu.00444.2016.
12. Pack, R.J., Al-Ugaily, L.H., and Widdicombe, J.G. (1984). The innervation of the trachea and extrapulmonary bronchi of the mouse. Cell Tissue Res. *238*, 61–68. https://doi.org/10.1007/BF00215145.
13. Korpás, J., and Kalocsayová, G. (1975). The expiration reflex in the mouse. Physiol. Bohemoslov. *24*, 253–256.
14. Sun, H., Lin, A.H., Ru, F., Patil, M.J., Meeker, S., Lee, L.Y., and Undem, B.J. (2019). KCNQ/M-channels regulate mouse vagal bronchopulmonary C-fiber excitability and cough sensitivity. JCI Insight *4*, e124467. https://doi.org/10.1172/jci.insight.124467.
15. Li, F., Jiang, H., Shen, X., Yang, W., Guo, C., Wang, Z., Xiao, M., Cui, L., Luo, W., Kim, B.S., et al. (2021). Sneezing reflex is mediated by a peptidergic pathway from nose to brainstem. Cell *184*, 3762–3773.e10. https://doi.org/10.1016/j.cell.2021.05.017.
16. Imamachi, N., Park, G.H., Lee, H., Anderson, D.J., Simon, M.I., Basbaum, A.I., and Han, S.K. (2009). TRPV1-expressing primary afferents generate behavioral responses to pruritogens via multiple mechanisms. Proc. Natl. Acad. Sci. USA *106*, 11330–11335.
17. Qu, L., Fan, N., Ma, C., Wang, T., Han, L., Fu, K., Wang, Y., Shimada, S.G., Dong, X., and LaMotte, R.H. (2014). Enhanced excitability of MRGPRA3- and MRGPRD-positive nociceptors in a model of inflammatory itch and pain. Brain *137*, 1039–1050. https://doi.org/10.1093/brain/awu007.
18. Liu, Q., Sikand, P., Ma, C., Tang, Z., Han, L., Li, Z., Sun, S., LaMotte, R.H., and Dong, X. (2012). Mechanisms of itch evoked by beta-alanine. J. Neurosci. *32*, 14532–14537. https://doi.org/10.1523/JNEUROSCI.3509-12.2012.
19. Hydén, D., and Arlinger, S. (2007). On the sneeze-reflex and its control. Rhinology *45*, 218–219.
20. Usoskin, D., Furlan, A., Islam, S., Abdo, H., Lönnerberg, P., Lou, D., Hjerling-Leffler, J., Haeggström, J., Kharchenko, O., Kharchenko, P.V., et al. (2015). Unbiased classification of sensory neuron types by large-scale single-cell RNA sequencing. Nat. Neurosci. *18*, 145–153. https://doi.org/10.1038/nn.3881.
21. Stantcheva, K.K., Iovino, L., Dhandapani, R., Martinez, C., Castaldi, L., Nocchi, L., Perlas, E., Portulano, C., Pesaresi, M., Shirlekar, K.S., et al. (2016). A subpopulation of itch-sensing neurons marked by Ret and somatostatin expression. EMBO Rep. *17*, 585–600. https://doi.org/10.15252/embr.201540983.
22. Peier, A.M., Moqrich, A., Hergarden, A.C., Reeve, A.J., Andersson, D.A., Story, G.M., Earley, T.J., Dragoni, I., McIntyre, P., Bevan, S., et al. (2002). A TRP channel that senses cold stimuli and menthol. Cell *108*, 705–715.
23. Bautista, D.M., Siemens, J., Glazer, J.M., Tsuruda, P.R., Basbaum, A.I., Stucky, C.L., Jordt, S.E., and Julius, D. (2007). The menthol receptor TRPM8 is the principal detector of environmental cold. Nature *448*, 204–208.
24. Chung, M.K., and Caterina, M.J. (2007). TRP channel knockout mice lose their cool. Neuron *54*, 345–347.
25. Colburn, R.W., Lubin, M.L., Stone, D.J., Jr., Wang, Y., Lawrence, D., D'Andrea, M.R., Brandt, M.R., Liu, Y., Flores, C.M., and Qin, N. (2007). Attenuated cold sensitivity in TRPM8 null mice. Neuron *54*, 379–386.
26. Doyle, W.J., Skoner, D.P., Seroky, J.T., Fireman, P., and Gwaltney, J.M. (1994). Effect of experimental rhinovirus 39 infection on the nasal response to histamine and cold air challenges in allergic and nonallergic subjects.

J. Allergy Clin. Immunol. *93*, 534–542. https://doi.org/10.1016/0091-6749(94)90364-6.

27. Cruz, A.A., and Togias, A. (2008). Upper airways reactions to cold air. Curr. Allergy Asthma Rep. *8*, 111–117.
28. Guan, Y., Liu, Q., Tang, Z., Raja, S.N., Anderson, D.J., and Dong, X. (2010). Mas-related G-protein-coupled receptors inhibit pathological pain in mice. Proc. Natl. Acad. Sci. USA *107*, 15933–15938.
29. Liu, Q., Weng, H.J., Patel, K.N., Tang, Z., Bai, H., Steinhoff, M., and Dong, X. (2011). The distinct roles of two GPCRs, MrgprC11 and PAR2, in itch and hyperalgesia. Sci. Signal. *4*, ra45. https://doi.org/10.1126/scisignal.2001925.
30. Reddy, V.B., Sun, S., Azimi, E., Elmariah, S.B., Dong, X., and Lerner, E.A. (2015). Redefining the concept of protease-activated receptors: cathepsin S evokes itch via activation of Mrgprs. Nat. Commun. *6*, 7864. https://doi.org/10.1038/ncomms8864.
31. Han, L., Ma, C., Liu, Q., Weng, H.J., Cui, Y., Tang, Z., Kim, Y., Nie, H., Qu, L., Patel, K.N., et al. (2013). A subpopulation of nociceptors specifically linked to itch. Nat. Neurosci. *16*, 174–182. https://doi.org/10.1038/nn.3289.
32. Liu, Q., Tang, Z., Surdenikova, L., Kim, S., Patel, K.N., Kim, A., Ru, F., Guan, Y., Weng, H.J., Geng, Y., et al. (2009). Sensory Neuron-Specific GPCR Mrgprs Are Itch Receptors Mediating Chloroquine-Induced Pruritus. Cell *139*, 1353–1365.
33. Liu, Y., Yang, F.C., Okuda, T., Dong, X., Zylka, M.J., Chen, C.L., Anderson, D.J., Kuner, R., and Ma, Q. (2008). Mechanisms of compartmentalized expression of Mrg class G-protein-coupled sensory receptors. J. Neurosci. *28*, 125–132. https://doi.org/10.1523/JNEUROSCI.4472-07.2008.
34. Liu, Q., Vrontou, S., Rice, F.L., Zylka, M.J., Dong, X., and Anderson, D.J. (2007). Molecular genetic visualization of a rare subset of unmyelinated sensory neurons that may detect gentle touch. Nat. Neurosci. *10*, 946–948.
35. Vrontou, S., Wong, A.M., Rau, K.K., Koerber, H.R., and Anderson, D.J. (2013). Genetic identification of C fibres that detect massage-like stroking of hairy skin in vivo. Nature *493*, 669–673. https://doi.org/10.1038/nature11810.
36. Elias, L.J., Succi, I.K., Schaffler, M.D., Foster, W., Gradwell, M.A., Bohic, M., Fushiki, A., Upadhyay, A., Ejoh, L.L., Schwark, R., et al. (2023). Touch neurons underlying dopaminergic pleasurable touch and sexual receptivity. Cell *186*, 577–590.e16. https://doi.org/10.1016/j.cell.2022.12.034.
37. Zylka, M.J., Dong, X., Southwell, A.L., and Anderson, D.J. (2003). Atypical expansion in mice of the sensory neuron-specific Mrg G protein-coupled receptor family. Proc. Natl. Acad. Sci. USA *100*, 10043–10048. https://doi.org/10.1073/pnas.1732949100.
38. Shinohara, T., Harada, M., Ogi, K., Maruyama, M., Fujii, R., Tanaka, H., Fukusumi, S., Komatsu, H., Hosoya, M., Noguchi, Y., et al. (2004). Identification of a G protein-coupled receptor specifically responsive to beta-alanine. J. Biol. Chem. *279*, 23559–23564.
39. Olson, W., Abdus-Saboor, I., Cui, L., Burdge, J., Raabe, T., Ma, M., and Luo, W. (2017). Sparse genetic tracing reveals regionally specific functional organization of mammalian nociceptors. eLife *6*, e29507. https://doi.org/10.7554/eLife.29507.
40. Alexander, G.M., Rogan, S.C., Abbas, A.I., Armbruster, B.N., Pei, Y., Allen, J.A., Nonneman, R.J., Hartmann, J., Moy, S.S., Nicolelis, M.A., et al. (2009). Remote control of neuronal activity in transgenic mice expressing evolved G protein-coupled receptors. Neuron *63*, 27–39. https://doi.org/10.1016/j.neuron.2009.06.014.
41. Guo, C., Jiang, H., Huang, C.C., Li, F., Olson, W., Yang, W., Fleming, M., Yu, G., Hoekel, G., Luo, W., et al. (2023). Pain and itch coding mechanisms of polymodal sensory neurons. Cell Rep. *42*, 113316. https://doi.org/10.1016/j.celrep.2023.113316.
42. Han, S.K., Dong, X., Hwang, J.I., Zylka, M.J., Anderson, D.J., and Simon, M.I. (2002). Orphan G protein-coupled receptors MrgA1 and MrgC11 are distinctively activated by RF-amide-related peptides through the Galpha q/11 pathway. Proc. Natl. Acad. Sci. USA *99*, 14740–14745. https://doi.org/10.1073/pnas.192565799.
43. Lembo, P.M., Grazzini, E., Groblewski, T., O'Donnell, D., Roy, M.O., Zhang, J., Hoffert, C., Cao, J., Schmidt, R., Pelletier, M., et al. (2002). Proenkephalin A gene products activate a new family of sensory neuron–specific GPCRs. Nat. Neurosci. *5*, 201–209.
44. Lee, M.G., Dong, X., Liu, Q., Patel, K.N., Choi, O.H., Vonakis, B., and Undem, B.J. (2008). Agonists of the MAS-related gene (Mrgs) orphan receptors as novel mediators of mast cell-sensory nerve interactions. J. Immunol. *180*, 2251–2255.
45. Bousquet, J., Van Cauwenberge, P., Bachert, C., Canonica, G.W., Demoly, P., Durham, S.R., Fokkens, W., Lockey, R., Meltzer, E.O., Mullol, J., et al. (2003). Requirements for medications commonly used in the treatment of allergic rhinitis. European Academy of Allergy and Clinical Immunology (EAACI), Allergic Rhinitis and its Impact on Asthma (ARIA). Allergy *58*, 192–197. https://doi.org/10.1034/j.1398-9995.2003.00054.x.
46. Howarth, P.H., Salagean, M., and Dokic, D. (2000). Allergic rhinitis: not purely a histamine-related disease. Allergy *55* (*Suppl 64*), 7–16.
47. Uzzaman, A., and Story, R. (2012). Chapter 5: Allergic rhinitis. Allergy Asthma Proc. *33* (*Suppl 1*), 15–18. https://doi.org/10.2500/aap.2012.33.3535.
48. Kushnir-Sukhov, N.M., Brown, J.M., Wu, Y., Kirshenbaum, A., and Metcalfe, D.D. (2007). Human mast cells are capable of serotonin synthesis and release. J. Allergy Clin. Immunol. *119*, 498–499. https://doi.org/10.1016/j.jaci.2006.09.003.
49. Huang, C.C., Yang, W., Guo, C., Jiang, H., Li, F., Xiao, M., Davidson, S., Yu, G., Duan, B., Huang, T., et al. (2018). Anatomical and functional dichotomy of ocular itch and pain. Nat. Med. *24*, 1268–1276. https://doi.org/10.1038/s41591-018-0083-x.
50. Binshtok, A.M., Bean, B.P., and Woolf, C.J. (2007). Inhibition of nociceptors by TRPV1-mediated entry of impermeant sodium channel blockers. Nature *449*, 607–610.
51. Xing, J., Weng, L., Yuan, B., Wang, Z., Jia, L., Jin, R., Lu, H., Li, X.C., Liu, Y.J., and Zhang, Z. (2016). Identification of a role for TRIM29 in the control of innate immunity in the respiratory tract. Nat. Immunol. *17*, 1373–1380. https://doi.org/10.1038/ni.3580.
52. Bin, N.R., Prescott, S.L., Horio, N., Wang, Y., Chiu, I.M., and Liberles, S.D. (2023). An airway-to-brain sensory pathway mediates influenza-induced sickness. Nature *615*, 660–667. https://doi.org/10.1038/s41586-023-05796-0.
53. Keeler, S.P., Agapov, E.V., Hinojosa, M.E., Letvin, A.N., Wu, K., and Holtzman, M.J. (2018). Influenza A Virus Infection Causes Chronic Lung Disease Linked to Sites of Active Viral RNA Remnants. J. Immunol. *201*, 2354–2368. https://doi.org/10.4049/jimmunol.1800671.
54. Fuller, R.W., Dixon, C.M., Cuss, F.M., and Barnes, P.J. (1987). Bradykinin-induced bronchoconstriction in humans. Mode of action. Am. Rev. Respir. Dis. *135*, 176–180. https://doi.org/10.1164/arrd.1987.135.1.176.
55. Katsumata, U., Sekizawa, K., Ujiie, Y., Sasaki, H., and Takishima, T. (1991). Bradykinin-induced cough reflex markedly increases in patients with cough associated with captopril and enalapril. Tohoku J. Exp. Med. *164*, 103–109. https://doi.org/10.1620/tjem.164.103.
56. Rahman, M.H., Bråtveit, M., and Moen, B.E. (2007). Exposure to ammonia and acute respiratory effects in a urea fertilizer factory. Int. J. Occup. Environ. Health *13*, 153–159. https://doi.org/10.1179/oeh.2007.13.2.153.
57. Wong, C.H., Matai, R., and Morice, A.H. (1999). Cough induced by low pH. Respir. Med. *93*, 58–61. https://doi.org/10.1016/s0954-6111(99)90078-1.
58. Aly, M., and Alotaibi, N.S. (2022). A novel deep learning model to detect COVID-19 based on wavelet features extracted from Mel-scale spectrogram of patients' cough and breathing sounds. Inform. Med. Unlocked *32*, 101049. https://doi.org/10.1016/j.imu.2022.101049.
59. Winterbauer, R.H., Ludwig, W.R., and Hammar, S.P. (1977). Clinical course, management, and long-term sequelae of respiratory failure due to influenza viral pneumonia. Johns Hopkins Med. J. *141*, 148–155.

60. Piirilä, P., and Sovijärvi, A.R. (1989). Differences in acoustic and dynamic characteristics of spontaneous cough in pulmonary diseases. Chest *96*, 46–53. https://doi.org/10.1378/chest.96.1.46.

61. Lakatos, H.F., Burgess, H.A., Thatcher, T.H., Redonnet, M.R., Hernady, E., Williams, J.P., and Sime, P.J. (2006). Oropharyngeal aspiration of a silica suspension produces a superior model of silicosis in the mouse when compared to intratracheal instillation. Exp. Lung Res. *32*, 181–199. https://doi.org/10.1080/01902140600817465.

62. Taylor-Clark, T.E., and Undem, B.J. (2022). Neural control of the lower airways: Role in cough and airway inflammatory disease. Handb. Clin. Neurol. *188*, 373–391. https://doi.org/10.1016/B978-0-323-91534-2.00013-8.

63. Huang, J., Polgár, E., Solinski, H.J., Mishra, S.K., Tseng, P.Y., Iwagaki, N., Boyle, K.A., Dickie, A.C., Kriegbaum, M.C., Wildner, H., et al. (2018). Circuit dissection of the role of somatostatin in itch and pain. Nat. Neurosci. *21*, 707–716. https://doi.org/10.1038/s41593-018-0119-z.

64. Huang, J., Polgár, E., Solinski, H.J., Mishra, S.K., Tseng, P.Y., Iwagaki, N., Boyle, K.A., Dickie, A.C., Kriegbaum, M.C., Wildner, H., et al. (2018). Author Correction: Circuit dissection of the role of somatostatin in itch and pain. Nat. Neurosci. *21*, 894. https://doi.org/10.1038/s41593-018-0149-6.

65. Datsi, A., Steinhoff, M., Ahmad, F., Alam, M., and Buddenkotte, J. (2021). Interleukin-31: The "itchy" cytokine in inflammation and therapy. Allergy *76*, 2982–2997. https://doi.org/10.1111/all.14791.

66. Lai, T., Wu, D., Li, W., Chen, M., Yi, Z., Huang, D., Jing, Z., Lü, Y., Lv, Q., Li, D., et al. (2016). Interleukin-31 expression and relation to disease severity in human asthma. Sci. Rep. *6*, 22835. https://doi.org/10.1038/srep22835.

67. Hallstrand, T.S., and Henderson, W.R., Jr. (2010). An update on the role of leukotrienes in asthma. Curr. Opin. Allergy Clin. Immunol. *10*, 60–66. https://doi.org/10.1097/ACI.0b013e32833489c3.

68. COVID-19 Investigation Team (2020). Clinical and virologic characteristics of the first 12 patients with coronavirus disease 2019 (COVID-19) in the United States. Nat. Med. *26*, 861–868. https://doi.org/10.1038/s41591-020-0877-5.

69. Wu, F., Zhao, S., Yu, B., Chen, Y.M., Wang, W., Song, Z.G., Hu, Y., Tao, Z.W., Tian, J.H., Pei, Y.Y., et al. (2020). A new coronavirus associated with human respiratory disease in China. Nature *579*, 265–269. https://doi.org/10.1038/s41586-020-2008-3.

70. Sikand, P., Dong, X., and LaMotte, R.H. (2011). BAM8-22 peptide produces itch and nociceptive sensations in humans independent of histamine release. J. Neurosci. *31*, 7563–7567. https://doi.org/10.1523/JNEUROSCI.1192-11.2011.

71. Zhang, L., Taylor, N., Xie, Y., Ford, R., Johnson, J., Paulsen, J.E., and Bates, B. (2005). Cloning and expression of MRG receptors in macaque, mouse, and human. Brain Res. Mol. Brain Res. *133*, 187–197.

72. Li, Z., Tseng, P.Y., Tiwari, V., Xu, Q., He, S.Q., Wang, Y., Zheng, Q., Han, L., Wu, Z., Blobaum, A.L., et al. (2017). Targeting human Mas-related G protein-coupled receptor X1 to inhibit persistent pain. Proc. Natl. Acad. Sci. USA *114*, E1996–E2005. https://doi.org/10.1073/pnas.1615255114.

73. Yu, H., Usoskin, D., Nagi, S.S., Hu, Y., Kupari, J., Bouchatta, O., Cranfill, S.L., Gautam, M., Su, Y., Lu, Y., et al. (2023). Single-Soma Deep RNA sequencing of Human DRG Neurons Reveals Novel Molecular and Cellular Mechanisms Underlying Somatosensation. Preprint at bioRxiv. https://doi.org/10.1101/2023.03.17.533207.

74. Nguyen, M.Q., von Buchholtz, L.J., Reker, A.N., Ryba, N.J., and Davidson, S. (2021). Single-nucleus transcriptomic analysis of human dorsal root ganglion neurons. eLife *10*, e71752. https://doi.org/10.7554/eLife.71752.

75. Tavares-Ferreira, D., Shiers, S., Ray, P.R., Wangzhou, A., Jeevakumar, V., Sankaranarayanan, I., Cervantes, A.M., Reese, J.C., Chamessian, A., Copits, B.A., et al. (2022). Spatial transcriptomics of dorsal root ganglia identifies molecular signatures of human nociceptors. Sci. Transl. Med. *14*, eabj8186. https://doi.org/10.1126/scitranslmed.abj8186.

76. Jung, M., Dourado, M., Maksymetz, J., Jacobson, A., Laufer, B.I., Baca, M., Foreman, O., Hackos, D.H., Riol-Blanco, L., and Kaminker, J.S. (2023). Cross-species transcriptomic atlas of dorsal root ganglia reveals species-specific programs for sensory function. Nat. Commun. *14*, 366. https://doi.org/10.1038/s41467-023-36014-0.

77. Yang, L., Xu, M., Bhuiyan, S.A., Li, J., Zhao, J., Cohrs, R.J., Susterich, J.T., Signorelli, S., Green, U., Stone, J.R., et al. (2022). Human and mouse trigeminal ganglia cell atlas implicates multiple cell types in migraine. Neuron *110*, 1806–1821.e8. https://doi.org/10.1016/j.neuron.2022.03.003.

78. Hamann, C.R., and Thyssen, J.P. (2018). Monoclonal antibodies against interleukin 13 and interleukin 31RA in development for atopic dermatitis. J. Am. Acad. Dermatol. *78* (*Suppl 1*), S37–S42. https://doi.org/10.1016/j.jaad.2017.12.018.

79. Nemoto, O., Furue, M., Nakagawa, H., Shiramoto, M., Hanada, R., Matsuki, S., Imayama, S., Kato, M., Hasebe, I., Taira, K., et al. (2016). The first trial of CIM331, a humanized antihuman interleukin-31 receptor A antibody, in healthy volunteers and patients with atopic dermatitis to evaluate safety, tolerability and pharmacokinetics of a single dose in a randomized, double-blind, placebo-controlled study. Br. J. Dermatol. *174*, 296–304. https://doi.org/10.1111/bjd.14207.

80. Pecova, T., Kocan, I., Vysehradsky, R., and Pecova, R. (2020). Itch and Cough - Similar Role of Sensory Nerves in Their Pathogenesis. Physiol. Res. *69* (*Suppl 1*), S43–S54. https://doi.org/10.33549/physiolres.934403.

81. Gibson, P.G. (2004). Cough is an airway itch? Am. J. Respir. Crit. Care Med. *169*, 1–2.

82. Mazzon, S.B., e, and Undem, B.J. (2016). Vagal Afferent Innervation of the Airways in Health and Disease. Physiol. Rev. *96*, 975–1024. https://doi.org/10.1152/physrev.00039.2015.

83. Forsberg, K., Karlsson, J.A., Theodorsson, E., Lundberg, J.M., and Persson, C.G. (1988). Cough and bronchoconstriction mediated by capsaicin-sensitive sensory neurons in the guinea-pig. Pulm. Pharmacol. *1*, 33–39. https://doi.org/10.1016/0952-0600(88)90008-7.

84. Zylka, M.J., Rice, F.L., and Anderson, D.J. (2005). Topographically distinct epidermal nociceptive circuits revealed by axonal tracers targeted to Mrgprd. Neuron *45*, 17–25.

85. McCoy, E.S., Taylor-Blake, B., and Zylka, M.J. (2012). CGRP$\alpha$-expressing sensory neurons respond to stimuli that evoke sensations of pain and itch. PLoS One *7*. e36355. https://doi.org/10.1371/journal.pone.0036355.

86. Li, F., Yang, W., Jiang, H., Guo, C., Huang, A.J.W., Hu, H., and Liu, Q. (2019). TRPV1 activity and substance P release are required for corneal cold nociception. Nat. Commun. *10*, 5678. https://doi.org/10.1038/s41467-019-13536-0.

87. Steele, H.R., Xing, Y., Zhu, Y., Hilley, H.B., Lawson, K., Nho, Y., Niehoff, T., and Han, L. (2021). MrgprC11$^{+}$ sensory neurons mediate glabrous skin itch. Proc. Natl. Acad. Sci. USA *118*, e2022874118. https://doi.org/10.1073/pnas.2022874118.

88. Zhao, Z.Q., Wan, L., Liu, X.Y., Huo, F.Q., Li, H., Barry, D.M., Krieger, S., Kim, S., Liu, Z.C., Xu, J., et al. (2014). Cross-inhibition of NMBR and GRPR signaling maintains normal histaminergic itch transmission. J. Neurosci. *34*, 12402–12414. https://doi.org/10.1523/JNEUROSCI.1709-14.2014.

89. Wan, L., Jin, H., Liu, X.Y., Jeffry, J., Barry, D.M., Shen, K.F., Peng, J.H., Liu, X.T., Jin, J.H., Sun, Y., et al. (2017). Distinct roles of NMB and GRP in itch transmission. Sci. Rep. *7*, 15466. https://doi.org/10.1038/s41598-017-15756-0.

90. Kim, Y.S., Chu, Y., Han, L., Li, M., Li, Z., Lavinka, P.C., Sun, S., Tang, Z., Park, K., Caterina, M.J., et al. (2014). Central Terminal Sensitization of TRPV1 by Descending Serotonergic Facilitation Modulates Chronic Pain. Neuron *81*, 873–887. https://doi.org/10.1016/j.neuron.2013.12.011.

91. Dhaka, A., Earley, T.J., Watson, J., and Patapoutian, A. (2008). Visualizing cold spots: TRPM8-expressing sensory neurons and their projections. J. Neurosci. *28*, 566–575. https://doi.org/10.1523/JNEUROSCI.3976-07.2008.

92. Panneton, W.M., Gan, Q., and Juric, R. (2006). Brainstem projections from recipient zones of the anterior ethmoidal nerve in the medullary dorsal

horn. Neuroscience *141*, 889–906. https://doi.org/10.1016/j.neuroscience.2006.04.055.

93. Kim, E.Y., Battaile, J.T., Patel, A.C., You, Y., Agapov, E., Grayson, M.H., Benoit, L.A., Byers, D.E., Alevy, Y., Tucker, J., et al. (2008). Persistent activation of an innate immune response translates respiratory viral infection into chronic lung disease. Nat. Med. *14*, 633–640. https://doi.org/10.1038/nm1770.

94. Wu, K., Byers, D.E., Jin, X., Agapov, E., Alexander-Brett, J., Patel, A.C., Cella, M., Gilfilan, S., Colonna, M., Kober, D.L., et al. (2015). TREM-2 promotes macrophage survival and lung disease after respiratory viral infection. J. Exp. Med. *212*, 681–697. https://doi.org/10.1084/jem.20141732.

95. Dell, R.B., Holleran, S., and Ramakrishnan, R. (2002). Sample size determination. ILAR J. *43*, 207–213.

## STAR★METHODS

### KEY RESOURCES TABLE

| REAGENT or RESOURCE | SOURCE | IDENTIFIER |
|---|---|---|
| **Antibodies** | | |
| Mouse anti-influenza A virus nucleoprotein | Abcam | Cat#ab20343; RRID: AB_445525 |
| Goat polyclonal anti-tdTomato | SICGEN | Cat#AB8181-200; RRID: AB_2722750 |
| Rabbit polyclonal anti-MrgprC11 | Proteintech Group | Cat#S3893-2 |
| Human HB-EGF (DTR) Antibody | R&D Systems | Cat#AF-259-NA; RRID: AB_354429 |
| Chicken anti-GFP | Aves | Cat#GFP-1020; RRID: AB_2307313 |
| Goat anti-WGA | Vector Laboratories | Cat#AS-2024; RRID: AB_2315608 |
| Guinea pig anti-Synaptophysin 1 | Synaptic System | Cat#101004; RRID: AB_1210382 |
| Goat anti-rabbit IgG-Alexa Fluor-488 | Invitrogen | Cat#A11008; RRID: AB_143165 |
| Goat anti-rabbit IgG-Alexa Fluor-555 | Invitrogen | Cat#A21429; RRID: AB_2535850 |
| Donkey anti-Mouse IgG (H+L)-Alexa Fluor™ 594 | Invitrogen | Cat#A21203; RRID: AB_141633 |
| Alexa Fluor® 488 AffiniPure F(ab')$_2$ Fragment Donkey Anti-Chicken IgY (IgG) (H+L) | Jackson Immuno Research | Cat#703546155; RRID: AB_2340376 |
| Alexa Fluor® 488 AffiniPure Donkey Anti-Goat IgG (H+L) | Jackson Immuno Research | Cat#705545147; RRID: AB_2336933 |
| Cy™3 AffiniPure Donkey Anti-Goat IgG (H+L) | Jackson Immuno Research | Cat#705165147; RRID: AB_2307351 |
| Cy™5 AffiniPure Donkey Anti-Guinea Pig IgG (H+L) | Jackson Immuno Research | Cat#706175148; RRID: AB_2340462 |
| **Bacterial and virus strains** | | |
| Influenza A virus (IAV) strain A/PR/8/34 | Michael J. Holtzman[53] | N/A |
| Influenza A virus (IAV) strain A/PR/8/34 | ATCC | VR-95 or VR-95PQ |
| Sendai virus (SeV) strain Sendai/52 Fushimi | ATCC | VR-105 |
| **Chemicals, peptides, and recombinant proteins** | | |
| β-alanine | Sigma | Cat#A9920; CAS: 107-95-9 |
| Ly344864 hydrochloride | Sigma | Cat#SML0556; CAS: 1217756-94-9 |
| Menthol | Sigma | Cat#M2780; CAS: 2216-51-5 |
| Chloroquine | Sigma | Cat#C6628; CAS: 50-63-5 |
| Capsaicin | Sigma | Cat#M2028; CAS: 404-86-4 |
| Histamine dihydrochloride | Sigma | Cat#H7250; CAS: 56-92-8 |
| Serotonin | Sigma | Cat#H9523; CAS: 153-98-0 |
| BAM (8-22) | Tocris | Cat#1763; CAS: 412961-36-5 |
| Neuropeptide FF | Bachem | Cat#H-5655.0001; CAS: 99566-27-5 |
| Neuropeptide FF | Tocris | Cat#3137; CAS: 99566-27-5 |
| Clozapine-N-Oxide | Tocris | Cat#4936; CAS: 34233-69-7 |
| Tamoxifen | Sigma | Cat#T5648; CAS: 10540-29-1 |
| Diphtheria Toxin | List labs | Cat#150 |
| Ovalbumin | Sigma | Cat#A5503; CAS: 9006-59-1 |
| Ammonia | Sigma | Cat#1054221000; CAS: 1336-21-6 |
| Citric acid | Sigma | Cat#251275; CAS: 77-92-9 |
| Bradykinin | Sigma | Cat#B3259; CAS: 6846-03-3 |
| IL-31 | PeproTech | Cat#200-31 |
| Evans Blue | Sigma | Cat#E2129; CAS: 314-13-6 |
| Somatostatin-Biotin Labeled | Phoenix Pharmaceuticals | Cat#B-060-03 |
| Streptavidin-ZAP | Advanced Targeting Systems | Cat#IT-27 |
| NMB-saporin | Advanced Targeting Systems | Cat#IT-70 |
| Blank-saporin | Advanced Targeting Systems | Cat#IT-21 |
| QX-314 | Sigma | Cat#L5783; CAS: 21306-56-9 |

(*Continued on next page*)

*Continued*

| REAGENT or RESOURCE | SOURCE | IDENTIFIER |
|---|---|---|
| Absolute Q DNA Digital PCR Master Mix | Applied Biosystems | Cat#A52490 |
| Corn oil | Sigma | Cat#C8267; CAS: 8001-30-7 |
| Avidin | Sigma | Cat#189727 |
| BCIP | Sigma | Cat#B6149; CAS: 102185-33-1 |
| NBT | Sigma | Cat#N6876; CAS: 298-83-9 |
| Bovine Serum Albumin | Fisher BioReagents | Cat#BP9706-100 |
| DAPI Fluoromount-G | Southern Biotech | Cat#0100-20 |
| Fluoromount-G | Southern Biotech | Cat#0100-01 |
| Imject Alum | ThermoFisher Scientific | Cat#77161 |
| Opal 520 | Akoya Biosciences | Cat#FP1487001KT |
| Opal 570 | Akoya Biosciences | Cat#FP1488001KT |
| PowerSYBR Green PCR Master Mix | Applied Biosystems | Cat#4367659 |
| Single Cell Lysis Buffer/Lysis Enhancer | Invitrogen | Cat#11739-010 |
| Trizol | Invitrogen | Cat#15596026 |
| WGA-Alexa Fluor 488 | Molecular Probes | Cat#W11261 |
| WGA-Alexa Fluor 555 | Molecular Probes | Cat#W32464 |
| HBSS | Gibco | Cat#14175079 |
| Dispase | Gibco | Cat#17105041 |
| Collagenase | Gibco | Cat#17100017 |
| DMEM/F12 | Gibco | Cat#11330032 |
| **Critical commercial assays** | | |
| High-Capacity cDNA Reverse Transcription Kit | Applied Biosystems | Cat#4368814 |
| RNAscope Multiplex Fluorescent V2 Assay kit | ACD Bio | Cat#323100 |
| Superscript III CellsDirect RT-PCR Kit | Invitrogen | Cat#18080-300 |
| **Experimental models: Organisms/strains** | | |
| Mouse: C57BL/6J | The Jackson Laboratory | Stock#000664 |
| Mouse: *Avil*$^{tm1(HBEGF)Phep/}$Cnrm (*Avil*$^{iDTR+}$) | European Mouse Mutant Archive | EMMA ID: 10409 |
| Mouse: B6N.129S1-*Mrgprb4*$^{tm3(cre)And}$/J | The Jackson Laboratory | Stock#021077 |
| Mouse: B6;129S6-*Gt(ROSA)26Sor*$^{tm9(CAG-tdTomato)Hze}$/J | The Jackson Laboratory | Stock#007905 |
| Mouse: B6N;129-Tg(CAG-CHRM3*,-mCitrine)1Ute/J | The Jackson Laboratory | Stock#026220 |
| Mouse: B6N.Cg-*Sst*$^{tm2.1(cre)Zjh}$/J | The Jackson Laboratory | Stock#018973 |
| Mouse: B6;129-*Gt(ROSA)26Sor*$^{tm2Nat}$/J | The Jackson Laboratory | Stock#009253 |
| Mouse: *Mrgpra3*$^{GFP\text{-}cre}$ | Xinzhong Dong[31] | N/A |
| Mouse: *Mrgprc11*$^{CreERT2}$ | Liang Han[87] | N/A |
| Mouse: *Mrgprd*$^{CreERT2/+}$ | Penn Gene Targeting Core and Laboratory (PGT) at the University of Pennsylvania | N/A |
| Mouse: *Mrgprd*$^{EGFPf/+}$ | David J Anderson[84] | N/A |
| Mouse: *Nmb*$^{flox/flox}$ | The Molecular Genetic Core at Washington University in St. Louis | N/A |
| Mouse: *Nmbr*$^{eGFP}$ | Zhou-feng Chen[88,89] | N/A |
| Mouse: *Pirt*$^{GCaMP3/+}$ | Xinzhong Dong[90] | N/A |
| Mouse: Trpm8$^{EGFPf/+}$ | Gina Story[91] | N/A |
| **Oligonucleotides** | | |
| Primers and probes for digital PCR | | N/A |
| Primer: InfA Forward: GTGCAGATGCAACGGTTCAA | Thermofisher | Custom |
| Primer: InfA Reverse: AGACTTTGGCACTCCTTCCG | Thermofisher | Custom |
| InfA Probe: ABY-AGGCCCTCCTTTCAGTCCGT-QSY | Thermofisher | Custom |

(*Continued on next page*)

| Continued | | |
|---|---|---|
| REAGENT or RESOURCE | SOURCE | IDENTIFIER |
| mm Actb Taqman assay (FAM/MGB) | Thermofisher | TAQMAN MM01205647_G1 |
| RNAscope Probe - Mm-Mrgprx1 | ACD Bio | Cat#488771 |
| RNAscope Probe - Mm-Nmb-C2 | ACD Bio | Cat#459931-C2 |
| RNAscope Probe - Mm-Mrgprd | ACD Bio | Cat#417921 |
| RNAscope Probe - Hs-CHRM3-No-XMm-O1-C2 | ACD Bio | Cat#1071861-C2 |
| RNAscope Probe - Mm-Sst-O1 | ACD Bio | Cat#482691 |
| Primers for single cell RT-qPCR, see Table S1 | This paper | N/A |
| Software and algorithms | | |
| FinePointe™ Software | DSI | 007898-001 Rev03 |
| Audacity | Audacity Team | https://www.audacityteam.org/ |
| MATLAB | Mathworks | https://www.mathworks.com/products/matlab.html |
| pCLAMP 10.5 | Molecular Devices | https://support.moleculardevices.com/s/article/Axon-pCLAMP-10-Electrophysiology-Data-Acquisition-Analysis-Software-Download-Page |
| Prism 9 | GraphPad | https://www.graphpad.com/scientific-software/prism/ |
| Other | | |
| Absolute Q Digital PCR System | Applied Biosystems | N/A |
| StepONE Real-Time PCR System | Applied Biosystems | N/A |
| Whole Body Plethysmography System | DSI | 601-1400-001 Rev11 |
| Ultrasonic Nebulizer | DSI | 08271-001 |
| Cryostat | Leica | CM-1950 |
| C2 confocal system | Nikon | N/A |
| Stereomicroscope | ZEISS | SteREO Discovery.V12 |
| Stereotaxic apparatus | Leica | 39477001 |
| Vibratome | Leica | VT1200 S |
| Video camera | Canon | VIXIA HFG10 |
| Micropipette puller | Sutter Instrument | P-1000 |
| MultiClamp 700B amplifier | Molecular Devices | N/A |
| Borosilicate glass capillaries | World Precision Instruments | 1B150F-4 |

## EXPERIMENTAL MODEL AND STUDY PARTICIPANT DETAILS

### Mouse lines

C57BL/6J wild-type (Stock#: 000664), B6N.129S1-*Mrgprb4*$^{tm3(cre)And}$/J (Stock#: 021077), B6;129S6-*Gt(ROSA)26Sor*$^{tm9(CAG-tdTomato)Hze}$/J (*ROSA26*$^{tdTomato}$; Stock#: 007905), B6N.Cg-*Sst*$^{tm2.1(cre)Zjh}$/J (Stock#: 018973), B6N;129-Tg(CAG-CHRM3*,-mCitrine)1Ute/J (Stock#: 026220), B6;129-*Gt(ROSA)26Sor*$^{tm2Nat}$/J (*ROSA26*$^{IAP}$, Stock#: 009253) mice were ordered from the Jackson Laboratory. *Avil*$^{tm1(HBEGF)Phep}$/Cnrm (*Avil*$^{iDTR+}$, EMMA ID: 10409) mice were ordered from European Mouse Mutant Archive (EMMA). *Mrgprd*$^{EGFPf/+}$ mice were from Dr. David J Anderson at the California Institute of Technology. *Mrgprd*$^{CreERT2/+}$ was generated by the Penn Gene Targeting Core and Laboratory (PGT) at the University of Pennsylvania. *Trpm8*$^{EGFPf/+}$ mice were gifted by Dr. Gina Story when she worked at Washington University Pain Center. *Mrgpra3*$^{GFP\text{-}cre}$ and *Pirt*$^{GCaMP3/+}$ mice were gifted by Dr. Xinzhong Dong at Johns Hopkins University. *Mrgprc11*$^{CreERT2}$ mice were generated by Dr. Liang Han when she worked at Dr. Xinzhong Dong's lab at Johns Hopkins University. *Nmb*$^{flox/flox}$ mice were produced using ES cells sourced from the European Conditional Mouse Mutagenesis Program (EUCOMM) by the Molecular Genetic Core at Washington University in St. Louis. *Nmbr*$^{eGFP}$ mice were from Dr. Zhou-Feng Chen when he worked at Washington University School of Medicine in St. Louis.[88,89] Animals used for behavioral experiments were backcrossed to the B6/J background. All mice used in this study were housed in temperature and humidity controlled vivarium with 12h:12h light/dark cycle and ad libitum access to food and water. All animal experiments were performed under protocols approved by the Institutional Animal Care and Use Committee at Washington University School of Medicine in St. Louis.

## METHOD DETAILS

### Histochemistry study of nasal tissues

Mice were anesthetized with ketamine/xylazine and transcardially perfused with ice cold PBS and 4% paraformaldehyde (PFA) in PBS (w/vol). The nose was dissected and post-fixed in 4% PFA on ice for 2 hours. Nasal tissues were then decalcified in EDTA solution (250 mM) in 30% sucrose/PBS for two days at 4°C, with buffer changes once every 12 hours. Following decalcification, nasal tissues were embedded in OCT (Sakura, 4583) and kept in a vacuum chamber for 2 hours to facilitate OCT penetration into the nasal cavity. Subsequently, the embedded nasal tissues were frozen and sectioned at 30 μm using a Leica CM-1950 cryostat.

For immunostaining, nose sections were blocked with 10% donkey serum in PBST (PBS containing 0.2% Triton X-100) for 1 hour, and incubated with primary antibodies overnight at 4°C. After washing, sections were then incubated with secondary antibodies for 2 hours at room temperature. Primary antibodies: chicken anti-GFP (Aves, GFP-1020; 1:1000 dilution), goat polyclonal anti-tdTomato (SICGEN, AB8181-200; 1:1000), mouse anti- influenza A virus nucleoprotein (Abcam, ab20343; 1:1000). Secondary antibodies: Alexa Fluor® 488 AffiniPure F(ab')$_2$ Fragment Donkey Anti-Chicken IgY (IgG) (H+L) (Jackson ImmunoResearch, 703546155; 1:500), Cy™3 AffiniPure Donkey Anti-Goat IgG (H+L) (Jackson ImmunoResearch, 705165147; 1:500), Donkey anti-Mouse IgG (H+L)-Alexa Fluor™ 594 (Invitrogen, A21203; 1:1000). After staining, sections were mounted using Fluoromount-G and imaged using a Nikon C2 confocal system.

### Retrograde labeling from nasal mucosa

Ketamine/xylazine anesthetized adult mice were positioned beneath a stereoscopic microscope, and ~2 μl WGA-Alexa Fluor 555 (5 mg/ml in PBS) was injected directly into the nasal mucosa using a fine glass capillary. Mice were used for immunofluorescence staining two days after injection.

### Retrograde labeling from the anterior ethmoidal nerve (AEN)

The AEN was identified and isolated using a previously published intracranial approach.[92] Briefly, animals were anesthetized using ketamine/xylazine, and the anterior cranial fossa was exposed by craniotomy under a microscope. The right side AEN was identified (traveling along the lower lateral side of the right olfactory bulb before entering the nasal mucosa) and approximately 500 nl WGA-Alexa Fluor 488 (5 mg/ml in PBS, Molecular Probes, Cat#W11261) or WGA-Alexa Fluor 555 (5 mg/ml in PBS, Molecular Probes, Cat#W32464) was injected into the nerve fiber using a fine glass capillary. Two days after the injection, the mouse trigeminal ganglia were used for single cell RT-qPCR or immunofluorescence staining.

### Retrograde labeling from the trachea

Mice were anesthetized with ketamine/xylazine and placed in a recumbent position. The trachea was exposed through making an incision on the anterior aspect of the neck. WGA-Alexa Fluor 488 or WGA-Alexa Fluor 555 (5 mg/ml in PBS) was injected into four discrete sites along the trachea (~500 nl/site) using a fine glass capillary. Three days after the injection, the mouse vagal sensory ganglia were used for single cell RT-qPCR or immunofluorescence staining.

### Single cell RT-qPCR

Single cell RT-qPCR was performed as described previously.[15,49] After retrograde labeling from the AEN or trachea, trigeminal ganglia and vagal sensory ganglia were collected, dissociated, and purified with a 15% BSA density gradient column. WGA marked neurons identified visually using an epifluorescence microscope, manually isolated, and collected into PCR tubes containing 10 μl of lysis buffer with 1 μl of lysis enhancer (Invitrogen 11739-010) and RNase inhibitor (Invitrogen, 18080-300). Isolated neurons were immediately frozen on dry ice and stored at -80°C until cDNA synthesis.

cDNA from single neurons were generated using Invitrogen SuperScript III CellsDirect cDNA Synthesis Kit (Invitrogen, 18080-300) following the protocol provided by the manufacturer. All samples underwent DNase treatment. Real-time PCR was performed using 2 μl of cDNA and PowerSYBR Green PCR Master Mix (Applied Biosystems 4367659) on an Applied Biosystems StepONE system. cDNA obtained from entire sensory ganglion lysate was used as a positive control. Single neuron genomic DNA was used as a negative control. All gene expression values are normalized to *Gapdh*, calculated using $2^{-(Ct(target\ Gene) - Ct(Gapdh))}$. Gene specific primers are listed in the Table S1.

### Sneezing behavior study

Mouse sneezing behavior was recorded using the Buxco Small Animal Whole Body Plethysmography System (DSI, 601-1400-001 Rev11) using protocols adapted from our previous publications.[15] Briefly, animals were placed into the WBP recording chambers for 10 to 40 minutes for acclimation and baseline testing. To induce sneezing, chemicals were either nebulized (DSI, 08271-001) into the testing chamber (300 μl over 2 minutes) or pipetted into the animal's nostrils. Cold air was administered by placing ice into the water supply port of the recording chamber in such a way so that local temperature stabilizes around 10°C. Sneezing responses were recorded for 5 or 10 min, and analysis was performed using the FinePointe™ Software (DSI, 007898-001 Rev03).

Nebulized chemicals: β-alanine (Sigma, A9920, 100 mM), $5HT_{1F}$ agonist Ly344864 hydrochloride (Sigma, SML0556, 1 mM), menthol (Sigma, M2780, 1 mM), chloroquine (sigma, C6628, 12 mM), capsaicin (Sigma, M2028, 12 μM), histamine (Sigma, H7250, 100 mM), and serotonin (Sigma, H9523, 1 mM).

Pipetted reagents: BAM (TOCRIS, 1763, 20 nmol in 2 μl saline), NPFF (BACHEM, H-5655.0001 or TOCRIS, 3137, 2 or 20 nmol in 2 μl saline), and Clozapine-N-Oxide (TOCRIS, 4936, 2 μl, 1 mM in 0.5% DMSO saline).

### Whole-cell patch clamp recordings of dissociated trigeminal neurons

The trigeminal ganglia (TG) were harvested from adult mice and placed in HBSS (Gibco, 14175079). TG were then digested with dispase (4U/ml, Gibco, 17105041) and collagenase (342 U/ml, Gibco, 17100017) in HBSS at 37 °C for 30 min. After enzymatic digestion, TG neurons were dissociated by gentle trituration, pelleted and resuspended. The neurons were seeded onto coverslips coated with poly-D-lysing and laminin, and cultured in DMEM/F12 medium (Gibco, 11330032) supplemented with 10% FBS and antibiotics at 37 °C in a humidified incubator with 95% air and 5% CO2 for 24 to 48 hours.

Whole-cell current-clamp recordings were performed using a MultiClamp 700B amplifier and pCLAMP 10.5 software (Molecular Devices). Patch pipettes were pulled from borosilicate glass capillaries (1B150F-4, World Precision Instruments) with a P-1000 horizontal puller (Sutter Instrument). The resistance of the patch pipettes was 3–5 MΩ when filled with an internal solution. Internal solution contained (in mM): $K^+$-gluconate 120, KCl 30, $MgCl_2$ 2, HEPES 10, MgATP 2, $CaCl_2$ 1, EGTA 11, with pH adjusted to 7.2 using Tris-base. During recording, coverslip with neurons were maintained at room temperature (22 ± 2 °C) in external solution containing (in mM): NaCl 145, KCl 3, $CaCl_2$ 2, $MgCl_2$ 2, glucose 10 and HEPES 10, pH 7.4. After stabilization, resting membrane potential (RMP) was recorded and neurons with RMP greater than -45 mV were omitted from the study.

### Itch behavioral testing

All behavioral tests were performed as described previously.[18,32] In short, 8 to 12-week-old transgenic mice, along with control littermates, were injected intradermally with Clozapine-N-Oxide (20 μl, 1 mM in 0.5% DMSO saline) at the right cheek. Test animals were then placed alone into their testing chambers and filmed. Scratches with the hind paw directed toward the injection site were scored for 30 min.

### Calcium imaging

For whole-mount calcium imaging of the nasal explants, nasal mucosa was rapidly dissected from 3-5 weeks old $Pirt^{GCaMP3/+}$ mice in ice cold external solution containing (in mM): NaCl 145, KCl 3, $CaCl_2$ 2, $MgCl_2$ 2, glucose 10 and HEPES 10, pH 7.4, and allowed to recover at room temperature for 20 min. Afterwards, dissected explants were transferred to the recording chamber and continuously perfused with external solution for 10 minutes. Calcium signals were acquired using a Nikon Ti-E inverted microscope and Photometrics CoolSnap HQ2 CCD camera (Tucson, AZ). Chemicals were either perfused into the recording chamber through a gravity-based delivery system (histamine and capsaicin) or bath applied (serotonin, NPFF and BAM). Nasal sensory fibers were visualized and analyzed using Nikon NIS Elements AR. Responses were defined as a minimum of 5% increase in GCaMP3 fluorescence intensity ($\Delta F/F_0$).

### Influenza infection model

Influenza A virus (IAV) strain A/PR/8/34 was obtained from either ATCC (VR-95 or VR-95PQ) or Dr. Michael J. Holtzman in the Department of Pulmonary and Critical Care Medicine at Washington University School of Medicine. Wild-type C57BL/6J mice (5-6 weeks old) were anesthetized with ketamine/xylazine and inoculated with IAV (1500 PFU in 5 μl / nostril). In the control group, WT mice were inoculated with an equivalent amount of UV-inactivated virus. Spontaneous sneezing behavior was recorded by WBP for 40 minutes at each of the indicated time points (12 h, 24 h, 36 h, 48 h, 60 h and 72 h) after viral inoculation. Body weights were measured daily.

To ablate MrgprC11$^+$ neurons, $Mrgprc11^{CreERT2+};Avil^{iDTR/+}$ mice and control littermates $Avil^{iDTR/+}$ were administered 40 mg/kg tamoxifen (Sigma, T5648) dissolved in corn oil (Sigma, C8267) by oral gavage for six consecutive days, starting at approximately P21. Three weeks after the completion of tamoxifen treatment, mice were given two intraperitoneal (*i.p.*) injections (three days apart) of 40 μg/kg of diphtheria toxin (DTX, List labs, 150) in saline. Three weeks after DTX treatment, mice were inoculated with IAV as described above.

To pharmacologically silence MrgprC11$^+$ nasal sensory fibers, 2 μl solution containing BAM (2 nmol) with or without 1% QX-314 (Sigma, L5783) was instilled into each nostril of tested mice at 24 h post-inoculation. Sneezing behavior was recorded at 30 min, 4 h, 8 h and 12 h afterwards.

### Digital PCR

Nasal mucosa, pharynx, larynx, trachea and lung were harvested and weighed at 36 h post-IVA infection. Total RNA was isolated using Trizol (Invitrogen, 15596026) and dissolved in 50 μl of RNase-free water. 1 μl RNA of each sample was reversely transcribed using an Applied Biosystems High-Capacity cDNA Reverse Transcription Kit (Applied Biosystems, 4368814) according to the manufacturer's instructions. cDNA was diluted 1:50, and 1 μl of the diluted cDNA was used for 10 μl dPCR reaction. Digital PCR was performed using Applied Biosystems Absolute Q DNA Digital PCR Master Mix (A52490) and an QuantStudio Absolute Q dPCR System. Genomic DNA was used as a negative control. Primers and probes are listed in key resources table.

### Whole-mount histochemistry staining

Fluorescent reporter mice were anesthetized using ketamine/xylazine and transcardially perfused with ice cold PBS followed by 4% PFA in PBS (w/vol). Nasal turbinate, nasal mucosa from the nasal wall, oropharynx, epiglottis, larynx and trachea were carefully

dissected and post-fixed in 4% PFA on ice for 15-30 min. For fluorescent tdTomato or GFP imaging, nasal tissues were directly mounted using Fluoromount-G after rinsing with PBS and imaged using Nikon C2 confocal system.

PLAP whole-mount histochemistry staining was performed as previously described.[87] Briefly, the adult *Mrgprc11*$^{CreERT2}$;*ROSA26*$^{IAP/+}$ mice were perfused with 4% PFA as described above, and tracheas were dissected and post-fixed in 4% PFA at 4°C for 2 hours. Dissected tissues were washed 3 times with B1 buffer (0.1 M Tris pH 7.5, 0.15 M NaCl) and 3 times with B3 buffer (0.1 M Tris pH 9.5, 0.1 M NaCl, 50 mM $MgCl_2$) before incubation in BCIP (37.5 μg/ml, Sigma, B6149) and NBT (175 μg/ml, Sigma, N6876) containing B3 buffer overnight at room temperature. Tissues were then fixed in 4% PFA at 4°C overnight and cleared in BABB (Benzyl Alcohol and Benzyl Benzoate, 1:2 mixture). Images were collected on a ZEISS SteREO Discovery.V12 stereomicroscope with a color camera.

For mast cell staining, whole-mount nasal tissues were incubated with fluorescein conjugated avidin (Millipore Sigma, 189727; 1:500) for 30 min at room temperature. After rinsing with PBS, nasal tissues were mounted using Fluoromount-G and imaged using Nikon C2 confocal system.

### Coughing behavior study

Mouse coughing behavior was recorded using the Buxco Small Animal Whole Body Plethysmography System (DSI, 601-1400-001 Rev11). For chemically-induced coughing, mice were lightly anesthetized by isoflurane and laid on their backs. Test solution (10 μl) was injected directly into the tracheas using a 30-gauged needle syringe with a 90° bend approximately 3 mm from the tip (Video S1). Tested reagents include ammonia solution (Sigma, 1054221000, 0.2%) with or without Evans blue (Sigma, E2129, 10%), citric acid (Sigma, 251275, 0.5 M), bradykinin (Sigma, B3259, 2.5 mg/ml), BAM (100 nmol in 10 μl saline), Clozapine-N-Oxide (1 mM in 0.5% DMSO saline), IL-31 (PeproTech, 200-31, 4 μM) and LY344864 hydrochloride (Sigma, SML0556, 1 mM). Coughing responses were recorded for 10-30 min.

To record audio of coughing and sneezing, a Zoom H4n Pro recorder (96 kHZ) was placed on the top of the recording chamber. Sound signals were analyzed using MATLAB.

### Oropharyngeal aspiration

Oropharyngeal aspiration was conducted as described previously.[61] Mice were lightly anesthetized by isoflurane and positioned on a commercially made intubation board. The mouse tongue was gently pulled out of the mouth with atraumatic forceps. Test solution was administered into the oropharynx while the nostrils was gently clamped and closed with atraumatic forceps. It forced mice breathe via mouth (gasp) within 30 sec and inhaled the experimental substance. Immediately after the gasp, the mouse nose and tongue were released, and normal nose breathing resumed. Mice recovered from anesthesia immediately. Tested reagents include saline, BAM (250 nmol in 25 μl saline) and LY344864 hydrochloride (25 nmol in 25 μl saline). Respiratory responses were recorded for 15 min.

### Neuronal ablation by SST-saporin and NMB-saporin

WT mice were anesthetized using ketamine/xylazine, and carefully positioned and secured in a stereotaxic apparatus (Leica, Model# 39477001) for the procedure. SST-saporin was customized by mixing biotin-labeled somatostatin (Phoenix Pharmaceuticals, Cat. #B-060-03) and Streptavidin-ZAP (Advanced Targeting Systems, Cat. #IT-27) at a 1:1 molar ratio at room temperature for 20 minutes. SST-Saporin (10 μM, 50 nL), NMB-saporin (Advanced Targeting Systems, Cat. #IT-70; 50 ng in 50 nL) or blank-saporin (Advanced Targeting Systems, Cat. #IT-21; 10 μM in 50 nL or 50 ng in 50 nL) was injected into the nucleus tractus solitarius (NTS) region via the following coordinates: anterior-posterior (AP) −7.55 mm, dorsoventral (DV) −4.35 mm, mediolateral (ML) ± 0.50 mm from bregma).

### Pulmonary fibrosis model

Sendai virus (SeV, Sendai/52 Fushimi strain, ATCC VR-105) was purchased from ATCC, and stocks were grown in embryonating chicken eggs, tittered by plaque-forming assay, and stored at -80°C as described previously.[93] Male C57BL/6J mice were purchased from Jackson Laboratory and inoculated intranasally with SeV or SeV-UV (UV-inactivated SeV) in 30 μl of PBS as described previously.[94] At day 49 post SeV infection, mouse lung tissue was collected for histopathology.

### Acute and chronic allergic rhinitis models

Mast cell-dependent allergy models were generated as described previously.[15] In short, an emulsion was prepared by combining 0.02% ovalbumin (OVA, Sigma, A5503) in sterile PBS (w/vol) with an equal volume of Imject Alum (Thermo Scientific, 77161). On the 1$^{st}$ and 11$^{th}$ day, mice were given *i.p.* injections of the OVA/Imject Alum mixture (200 μl). In the acute allergy model, sneezing behavior was recorded for 10 min after challenge with intranasal instillation of OVA (10%, 2 μl) on day 14. In the chronic allergy model, sensitized mice were given daily intranasal OVA (10%, 2 μl) challenges under isoflurane anesthesia for five consecutive days (from day 14 to 18). Sneezing behavior was tested immediately after nasal challenge with OVA (10%, 2 μl) on day 19.

To pharmacologically silence MrgprC11$^+$ nasal sensory fibers, 2 μl mixture solution containing 2 nmol BAM and/or 1% QX-314 was instilled into each nostril of tested mice 30 min before OVA challenge. Sneezing responses were recorded for 10 min after OVA treatment.

### *In Situ* Hybridization

Fluorescent *In Situ* Hybridization (FISH) was performed using the RNAscope Multiplex Fluorescent V2 Assay kit (ACD Bio, 323100) and a procedure adapted from the manufacturer's recommended protocol. Briefly, animals were euthanized by $CO_2$ asphyxiation and transcardially perfused with ice cold PBS to quickly lower tissue temperature. Trigeminal and DRG tissues were immediately dissected, frozen in OCT, and sectioned and slide mounted using a Leica CM-1950 cryostat. Slides were dried in a -20°C freezer for 1 hour before fixation in ice cold 4% PFA for 15 minutes. After fixation, slides were rinsed in two 2-min PBS washes before dehydration, $H_2O_2$ quenching, and antigen retrieval according to the manufacturer's protocol. After antigen retrieval, slides were dehydrated again, dried in a 60°C desiccating oven for 5 minutes, and room temperature overnight before protease treatment and probe hybridization. Signal development was performed using the manufacture's recommended protocol and Opal 520 and 570 fluorophore reagents (Akoya Biosciences, FP1487001KT and FP1488001KT respectively). Slides were mounted using DAPI Fluoromount-G (SouthernBiotech, 0100-20), dried at 4°C overnight before imaging. Total processing time between animal sacrifice and mounting was no more than 28 hours. Probes used are listed in the key resources table.

### Immunofluorescence staining of the sensory ganglia and the brainstem

Ketamine/xylazine anesthetized adult mice were transcardially perfused with ice cold PBS followed by 4% PFA. Trigeminal ganglia (TG), vagal sensory ganglia (VG) and brainstems were harvested and post-fixed in the same fixative for 30 min (for ganglia) and 4-6 hours (for the brainstems) on ice, respectively. After post-fixation, tissues were cryoprotected in 30% (w/v) sucrose for one night (for ganglia) or two nights (for the brainstems) at 4°C, embedded and frozen in OCT. TGs and VGs were sectioned at 12 μm onto slides and brainstems were sectioned at 50 μm for free-floating section staining using a cryostat. Sectioned tissues were stained and imaged as described in the previous section. Primary antibodies: rabbit polyclonal anti-MrgprC11 (custom-made by Proteintech Group, S3893-2; 1:1000), Human HB-EGF (DTR) Antibody (R&D Systems, AF-259-NA; 1:1000), chicken anti-GFP (Aves, GFP-1020; 1:1000), goat anti-WGA (Vector Laboratories, AS-2024; 1:1000), guinea pig anti-Synaptophysin 1 (Synaptic System, 101004, Lot# 3-38; 1:200). Secondary antibodies: goat anti-rabbit IgG-Alexa Fluor-488 (Invitrogen, A11008; 1:500), goat anti-rabbit IgG-Alexa Fluor-555 (Invitrogen, A21429; 1:500), Alexa Fluor® 488 AffiniPure F(ab')₂ Fragment Donkey Anti-Chicken IgY (IgG) (H+L) (Jackson ImmunoResearch, 703546155; 1:500), Cy™3 AffiniPure Donkey Anti-Goat IgG (H+L) (Jackson ImmunoResearch, 705165147; 1:500), Alexa Fluor® 488 AffiniPure Donkey Anti-Goat IgG (H+L) (Jackson ImmunoResearch, 705545147; 1:500), Cy™5 AffiniPure Donkey Anti-Guinea Pig IgG (H+L) (Jackson ImmunoResearch, 706175148; 1:500).

### Brainstem slice preparation and electrophysiological recordings

As described previously,[15] *Nmbr*$^{eGFP}$ mice aged between 14 and 21 days were deeply anesthetized using isoflurane and decapitated at the level of the cervical spine. The brainstem was quickly collected and immersed in ice cold solution containing (in mM): Sucrose 209, KCl 2, $NaH_2PO_4$ 1.25, $MgCl_2$ 5, $CaCl_2$ 0.5, $NaHCO_3$ 26 and glucose 10, bubbled with 95% $O_2$, 5% $CO_2$. Brainstems were then horizontally embedded in agar and sagittal slices (350 μm per slice) were made using a Vibratome (Leica VT1200 S). Slices were incubated at 34°C for 30 min for recovery in holding artificial cerebrospinal fluid (ACSF) solution containing (in mM): NaCl 92, KCl 2.5, $NaH_2PO_4$ 1.25, $NaHCO_3$ 30, $MgCl_2$ 2, $CaCl_2$ 2, glucose 25 and HEPES 20, bubbled with 95% $O_2$, 5% $CO_2$. Before recording, slices were placed at room temperature at least one hour. After incubation, slices were transferred to a recording chamber and continuously perfused with oxygenated recording ACSF solution containing (in mM): NaCl 124, KCl 2.5, $NaH_2PO_4$ 1.25, $NaHCO_3$ 24, $MgCl_2$ 1, $CaCl_2$ 2, glucose 12.5 and HEPES 5. Whole-cell current-clamp recordings were then conducted on NMBR$^+$ neurons in the sneeze-evoking region of brainstem slices with a MultiClamp 700B amplifier and pCLAMP 10.5 software (Molecular Devices). Patch pipettes were pulled from borosilicate glass capillaries (1B150F-4, World Precision Instruments) using a horizontal micropipette puller (Model P-1000, Sutter Instrument). The resistance of the patch pipettes were 5-7 MΩ when filled with the internal solution containing (in mM): $K^+$-gluconate 130, NaCl 10, $MgCl_2$ 1, EGTA 0.2, HEPES10, Mg-ATP 1, Na-GTP 5 at an osmolarity of 290–300 mOsm and a pH adjusted to 7.25 with KOH.

## QUANTIFICATION AND STATISTICAL ANALYSIS

All data in graphs are presented as the mean ± s.e.m. The sample sizes were selected based on ''Sample size determination''[95], our pilot studies, relevant prior studies, and other considerations including technical restraints, resource availability, and ethical use. Unless stated otherwise, n numbers in all figure legends indicate biological replicates. All statistical analysis were conducted using Prism 9 (GraphPad, San Diego, CA). Two-tailed Student's t tests were conducted to determine statistical significance between two groups. One-way ANOVA and Tukey-Kramer post hoc tests were used for comparisons involving three or more groups. The threshold for statistically significant between groups was set at $P \leq 0.05$.

CellPress
OPEN ACCESS

# Supplemental figures

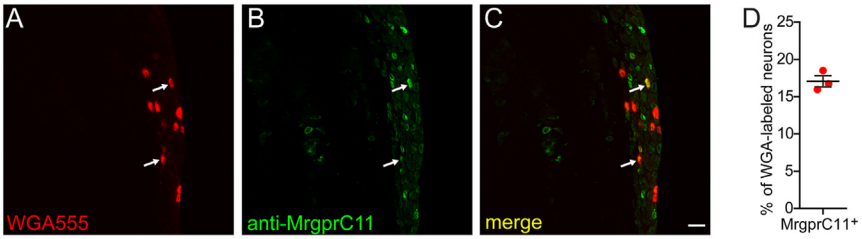


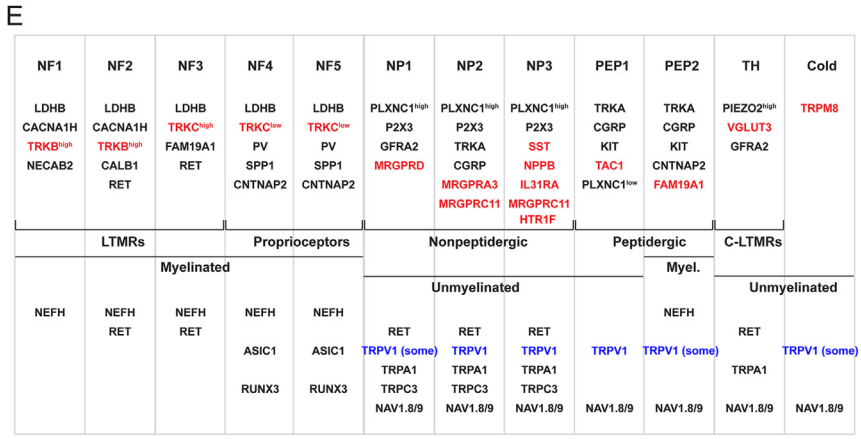


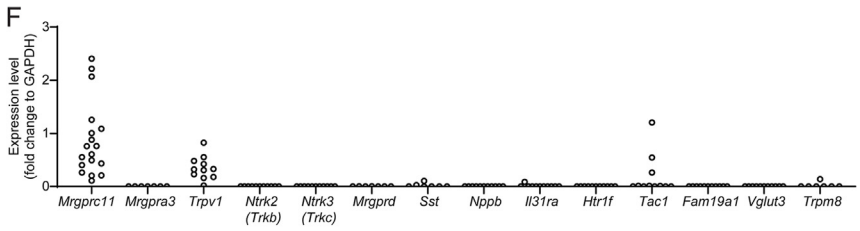


**Figure S1. Characterization of nasal MrgprC11$^+$ sensory neurons, related to Figure 1**

(A–D) The retrograde labeling of nasal sensory neurons using wheat germ agglutinin conjugated with Alexa Fluor 555 (WGA555). Arrows indicate MrgprC11$^+$ neurons (green, B and C) labeled by WGA555 (red, A and C) in the section of the trigeminal ganglion. (D) Shows the proportion of WGA-labeled nasal sensory neurons that express MrgprC11.

(E) The classification of primary sensory neuron (modified based on Usoskin et al.[20]). Molecular markers for discrete neuronal populations are highlighted in red. TRPV1 expression by multiple sensory populations was revealed by previous studies (Usoskin et al.[20]; Zylka et al.[84]; McCoy et al.[85]; Li et al.[86]).

(F) Single-cell RT-qPCR of nasal sensory neurons retrogradely labeled from the anterior ethmoidal nerve. As a subset of nasal TRPV1$^+$ sensory neurons, MrgprC11$^+$ MrpgrA3$^-$ neurons do not express most molecular markers of other sensory populations examined. A small subset of MrgprC11$^+$ nasal sensory neurons (3 out of 11 neurons) express *Tac1*, a molecular marker for the peptidergic PEP1 population. However, PEP1 population does not express *Mrgprc11* or *P2rx3*, and are discrete from MrgprC11$^+$ sensory neurons. Each dot represents one sensory neuron. Data are presented as mean ± SEM. All images shown are representative of three biological replicates. Scale bar, 50 μm.

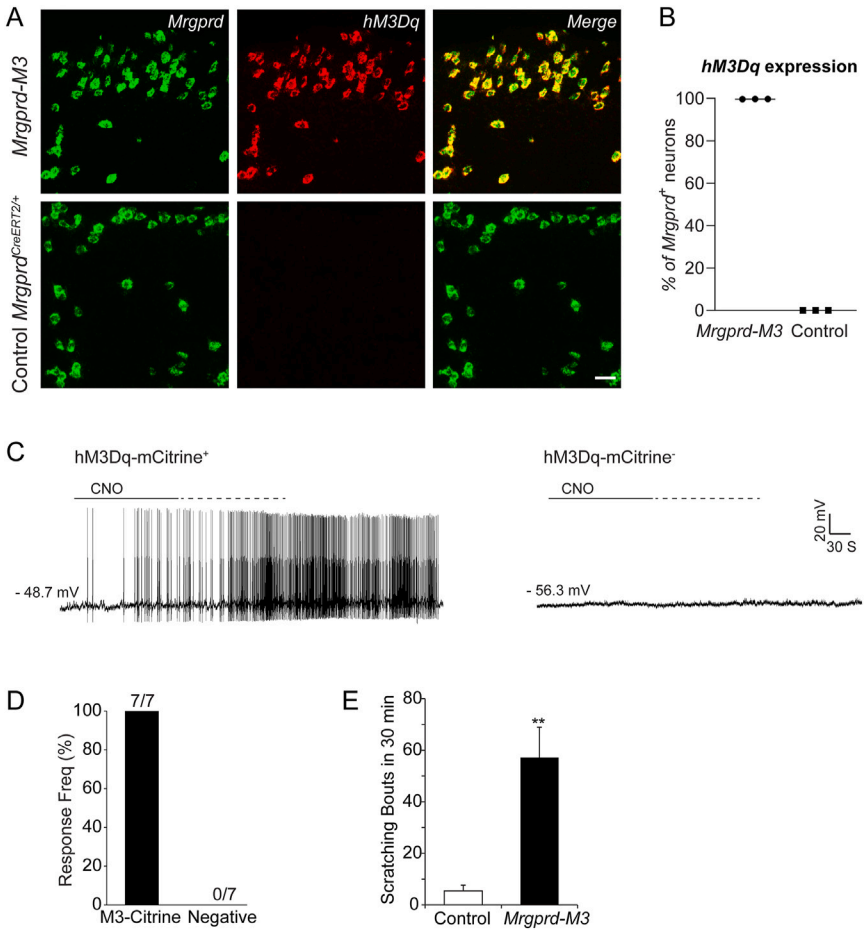


**Figure S2. Characterization of *Mrgprd*$^{CreERT2/+}$; *Tg*$^{CAG\text{-}LSL\text{-}Gq\text{-}DREADD(hM3Dq)\text{-}mCitrine}$ (*Mrgprd-M3*) mice, related to Figure 2**

(A) Representative images showing RNAscope *in situ* hybridization for *Mrgprd* (green) and *hM3Dq* mRNA (red) in the trigeminal ganglia of *Mrgprd-M3* and control *Mrgprd*$^{CreERT2/+}$ mice after tamoxifen induction.

(B) Shows the proportion of *Mrgprd*$^{+}$ sensory neurons that co-express *hM3Dq* mRNA in *Mrgprd-M3* and control *Mrgprd*$^{CreERT2/+}$ mice. Each dot represents an individual mouse.

(C) Whole-cell current clamp recordings of cultured hM3Dq-mCitrine$^{+}$ and hM3Dq-mCitrine$^{-}$ trigeminal neurons from *Mrgprd-M3* mice. Traces are representative of neuronal responses to bath-applied clozapine-N-oxide (CNO, 100 μM).

(D) Quantification of CNO responses in cultured trigeminal neurons from *Mrgprd-M3* mice ($n$ = 3).

(E) Cheek intradermal injection of CNO (20 nmol in 20 μL) produced robust itch-related scratching behavior in *Mrgprd-M3* mice, but not in control mice. Data are presented as mean ± SEM. ** $p \leq 0.01$. All images shown are representative of three biological replicates. Scale bar, 50 μm.

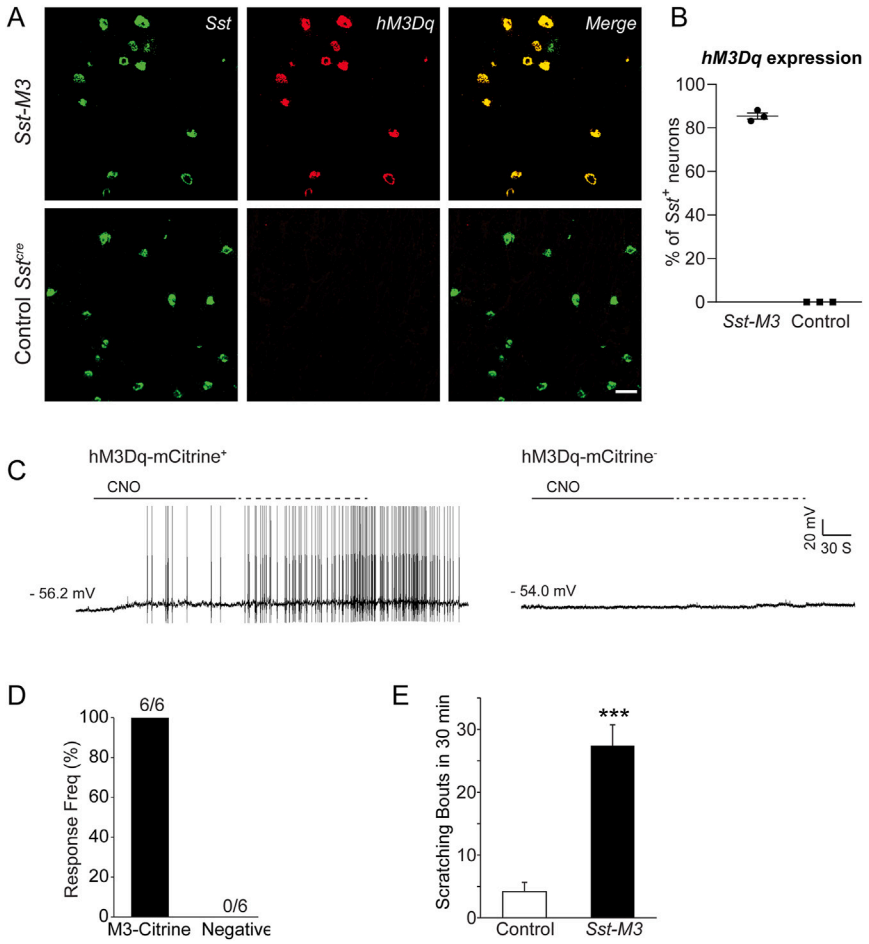


**Figure S3. Characterization of *Sst*$^{Cre/+}$; *Tg*$^{CAG\text{-}LSL\text{-}Gq\text{-}DREADD(hM3Dq)\text{-}mCitrine}$ (*Sst-M3*) mice, related to Figure 2**

(A) Representative images showing RNAscope *in situ* hybridization for *Sst* (green) and *hM3Dq* mRNA (red) in the trigeminal ganglia of *Sst-M3* and control *Sst*$^{Cre/+}$ mice.

(B) Shows the proportion of *Sst*$^{+}$ sensory neurons that co-express *hM3Dq* mRNA in *Sst-M3* and control *Sst*$^{Cre/+}$ mice. Each dot represents an individual mouse.

(C) Whole-cell current clamp recordings of cultured hM3Dq-mCitrine$^{+}$ and hM3Dq-mCitrine$^{-}$ trigeminal neurons from *Sst-M3* mice. Traces are representative of neuronal responses to bath-applied clozapine-N-oxide (CNO, 100 μM).

(D) Quantification of CNO responses in cultured trigeminal neurons from *Sst-M3* mice ($n$ = 3).

(E) Cheek intradermal injection of clozapine-N-oxide (CNO, 20 nmol in 20 μL) generated significant itch-related scratching behavior in *Sst*$^{Cre/+}$; *Tg*$^{CAG\text{-}LSL\text{-}Gq\text{-}DREADD(hM3Dq)}$ (*Sst-M3*) mice, but not in control *Sst*$^{Cre/+}$ mice. Data are presented as mean ± SEM. *** $P \leq 0.001$. All images shown are representative of three biological replicates. Scale bar, 50 μm.

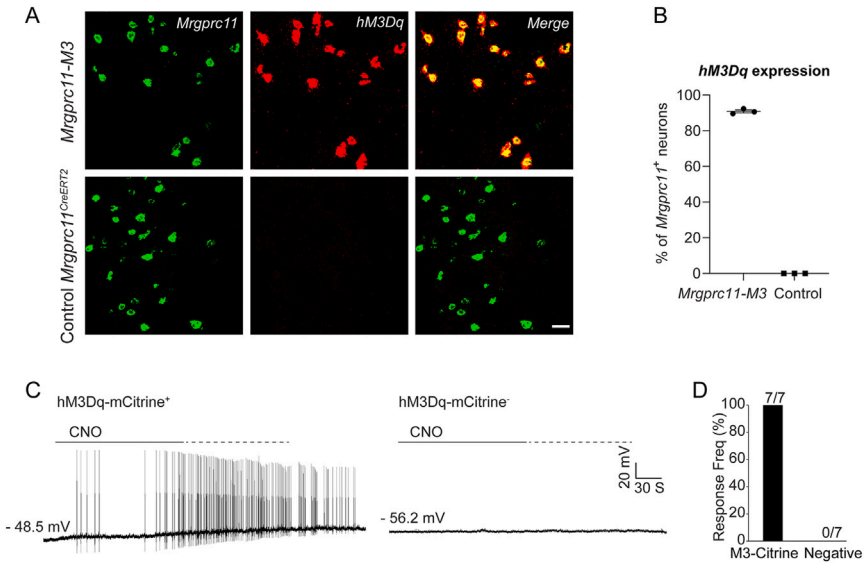


**Figure S4. Characterization of *Mrgprc11*$^{CreERT2}$; *Tg*$^{CAG\text{-}LSL\text{-}Gq\text{-}DREADD(hM3Dq)\text{-}mCitrine}$ (*Mrgprc11-M3*) mice, related to Figure 2**

(A) Representative images showing RNAscope *in situ* hybridization for *Mrgprc11* (green) and *hM3Dq* mRNA (red) in the trigeminal ganglia of *Mrgprc11-M3* and control *Mrgprc11*$^{CreERT2}$ mice after tamoxifen induction.

(B) Shows the proportion of *Mrgprc11*$^{+}$ sensory neurons that co-express *hM3Dq* mRNA in *Mrgprc11-M3* and control *Mrgprc11*$^{CreERT2}$ mice. Each dot represents an individual mouse.

(C) Whole-cell current clamp recordings of cultured hM3Dq-mCitrine$^{+}$ and hM3Dq-mCitrine$^{-}$ trigeminal neurons from *Mrgprc11-M3* mice. Traces are representative of neuronal responses to bath-applied clozapine-N-oxide (CNO, 100 μM).

(D) Quantification of CNO responses in cultured trigeminal neurons from *Mrgprc11-M3* mice ($n$ = 3). Data are presented as mean ± SEM. All images shown are representative of three biological replicates. Scale bar, 50 μm.

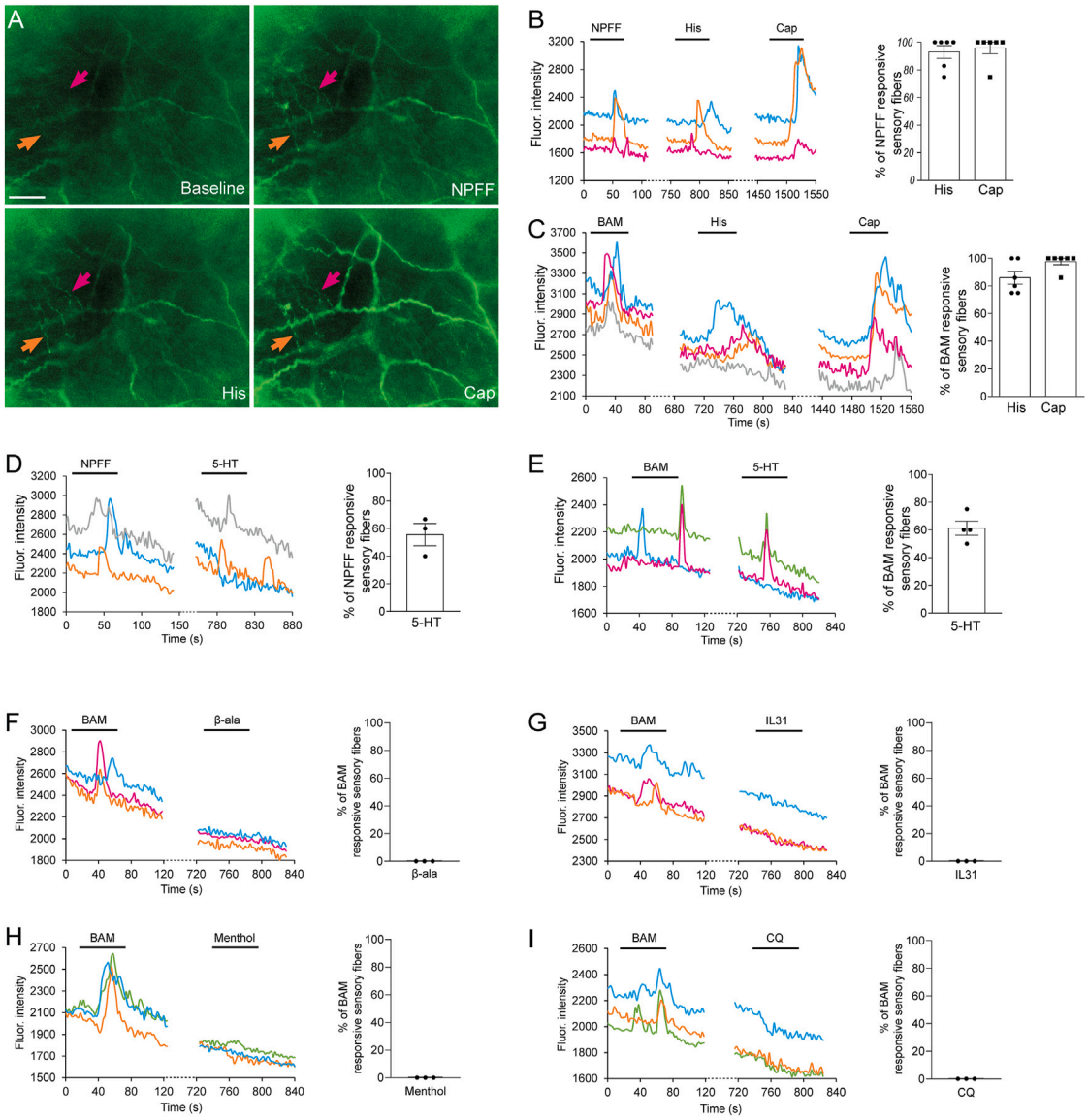


**Figure S5. Nasal MrgprC11$^{+}$ sensory fibers are sensitive to a variety of sneeze-inducing stimuli and constitute a physiologically defined population, related to Figure 3**

(A) Representative *ex vivo* calcium imaging of whole-mount nasal mucosa shows that nasal MrgprC11$^{+}$ sensory fibers (marked by the sensitivity to MrgprC11 agonist NPFF [20 μM]) can be activated by various sneeze-inducing stimuli, including histamine (His, 10 mM) and capsaicin (Cap, 10 μM), as revealed by the fluorescence changes of GCaMP3 in *Pirt*$^{GCaMP3/+}$ mice.

(B–E) Representative $Ca^{2+}$ transients of nasal sensory fibers upon stimulation with MrgprC11 agonists NPFF or BAM 8-22 (20 μM) and other sneeze-inducing stimuli, including histamine, capsaicin, and serotonin (5-HT, 100 μM). Bar graphs show the proportion of MrgprC11 agonist-sensitive nasal sensory fibers that were activated by other sneeze-inducing stimuli.

(F–I) Nasal MrgprC11$^{+}$ sensory fibers (identified by BAM sensitivity) do not respond to β-alanine (1 mM), IL-31 (300 nM), menthol (1 mM), and CQ (1 mM). Notably, these chemicals activate nasal neuronal populations other than MrgprC11$^{+}$ neurons, but do not induce significant sneezing in mice (see Figure 2). Data are presented as mean ± SEM. Each dot represents a nasal mucosa explant from *Pirt*$^{GCaMP3/+}$ mouse ($n$ = 3–6/group). All images shown are representative of three biological replicates. Scale bar, 20 μm.

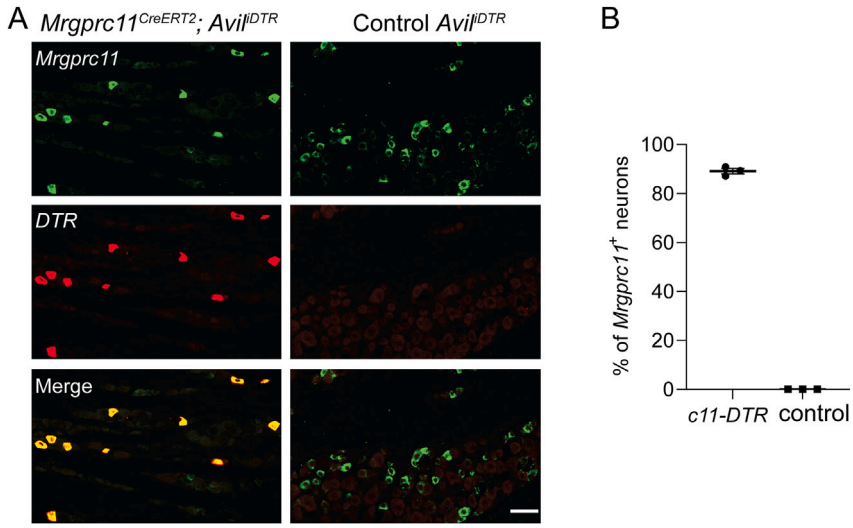


**Figure S6. Characterization of *Mrgprc11$^{CreERT2}$; Avil-$^{DTR}$* mice, related to Figure 3**

(A) Representative images showing fluorescent immunostaining for MrgprC11 (green) and the primate diphtheria toxin receptor (DTR, red) in the trigeminal ganglia of *Mrgprc11$^{CreERT2}$; Avil-$^{DTR}$* and control *Avil-$^{DTR}$* mice after tamoxifen induction.

(B) Shows the proportion of MrgprC11$^{+}$ sensory neurons that co-express DTR in *Mrgprc11$^{CreERT2}$; Avil-$^{DTR}$* and control *Avil-$^{DTR}$* mice. Each dot represents an individual mouse. Data are presented as mean ± SEM. All images shown are representative of three biological replicates. Scale bar, 50 μm.

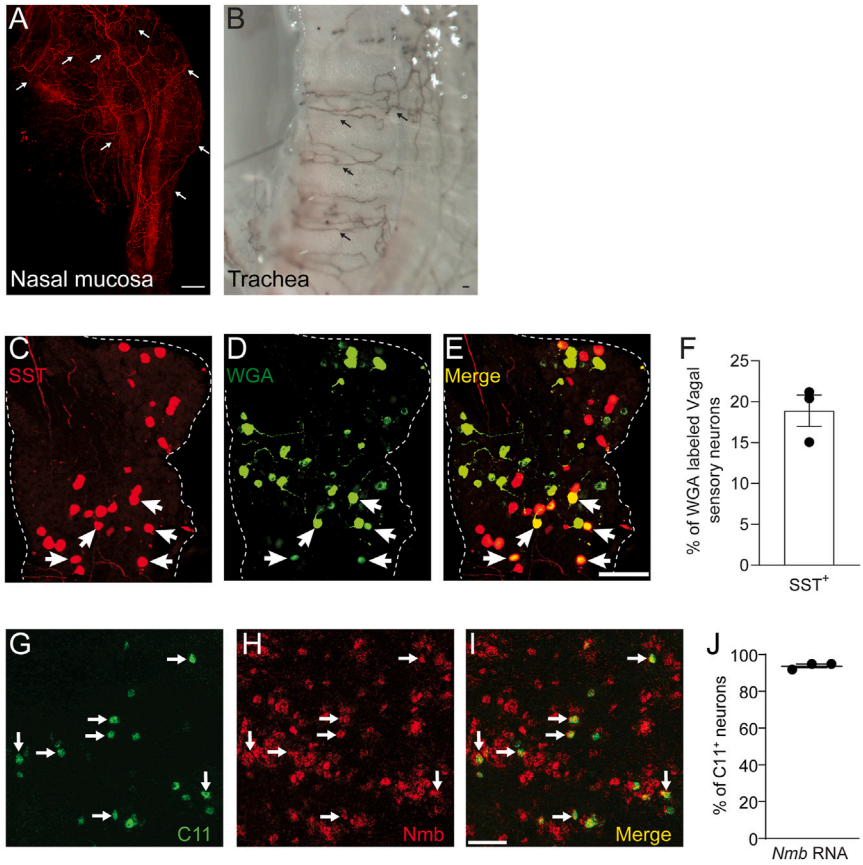


**Figure S7. Characterization of airway sensory innervations, related to Figures 6 and 7**

(A and B) MrgprC11$^{+}$ sensory fiber innervation in the nasal mucosa (indicated by arrows in A, *Mrgprc11*$^{CreERT2}$*; ROSA26*$^{tdTomato/+}$ mice) and the trachea (indicated by arrows in B, *Mrgprc11*$^{CreERT2}$*; ROSA26*$^{PLAP/+}$ mice), as revealed by whole-mount staining.

(C–F) The retrograde labeling of tracheal sensory neurons using wheat germ agglutinin (WGA) conjugated with Alexa Fluor 488. Arrows indicate SST-tdTomato neurons (red) labeled by WGA (green) in the section of the vagal sensory ganglion from *Sst*$^{Cre/+}$*; ROSA26*$^{tdTomato/+}$ reporter line. The graph shows the proportion of WGA-labeled tracheal sensory neurons that express SST-tdTomato.

(G–J) MrgprC11$^{+}$ sensory neurons express neuromedin B (NMB) peptide. (G–I) Representative images showing RNAscope *in situ* hybridization for *Mrgprc11* (green) and *Nmb* mRNA (red) in the V1 division of the trigeminal ganglia (TG) of WT mice. (J) Shows the proportion of MrgprC11$^{+}$ sensory neurons that co-express *Nmb* mRNA. Each dot represents an individual WT mouse. Data are presented as mean ± SEM. All images shown are representative of three biological replicates. Scale bars, 100 μm.